

# Adsorption and Decomposition of Methanol on Gallium Oxide Polymorphs

Sebastián E. Collins,<sup>†</sup> Laura E. Briand,<sup>‡</sup> Luis A. Gambaro,<sup>‡</sup> Miguel A. Baltanás,<sup>†</sup> and Adrian L. Bonivardi<sup>\*,†</sup>

*Instituto de Desarrollo Tecnológico para la Industria Química, CONICET, Universidad Nacional del Litoral, Güemes 3450, S3000GLN Santa Fe, Argentina and Centro de Investigación y Desarrollo en Ciencias Aplicadas, CONICET-Universidad Nacional de La Plata, Calle 47 No. 257, B1900AJK La Plata, Argentina*

*Received: February 12, 2008; Revised Manuscript Received: June 27, 2008*

The adsorption of methanol was studied on three gallia polymorphs ( $\alpha$ ,  $\beta$ , and  $\gamma$ ), pretreated under oxygen or hydrogen at 723 K. Their Brunauer–Emmett–Teller surface areas were in the range 12–105 m<sup>2</sup> g<sup>-1</sup>. Methanol (or methanol-d<sub>3</sub>) chemisorbs on the gallium oxides both molecularly, as CH<sub>3</sub>OH<sub>s</sub> (or CD<sub>3</sub>OH<sub>s</sub>) and dissociatively, as methoxy (CH<sub>3</sub>O or CD<sub>3</sub>O) species, at 373 K. The quantification of the total amount of chemisorbed methanol at this temperature allowed us to determine the number of available surface active sites per unit area ( $N_s$ ), which is in the range 1–2  $\mu$ mol m<sup>-2</sup> for the oxygen pretreated oxides at 723 K. The density of active sites was moderately smaller (~25%) after pretreating the oxides under hydrogen at 723 K. The temperature-programmed surface reaction of adsorbed methanol and methoxy was followed by mass spectrometry and infrared spectroscopy under He flow, up to 723 K. It was found that, upon heating above 473 K, methoxy oxidized to methylenbisoxi (H<sub>2</sub>COO) and, then, to formate (HCOO) species, and traces of dimethyl ether were also detected. Surface formate species further decompose to give CO(g) and CO<sub>2</sub>(g) at temperatures higher than 573 K, with the concurrent generation of OH and H species over the surface, which react toward H<sub>2</sub>(g). It is suggested that the CO<sub>2</sub> production implies the removal of lattice oxygen, generating a surface oxygen vacancy, which can be restored by water molecules from the gas phase. Thus, gallia can be envisaged as a promising support for the steam reforming of methanol, as long as a (noble) metal officiates/acts as a rapid H<sub>2</sub> releaser from the surface.

## 1. Introduction

It has been shown along the last two decades that gallium-containing catalysts are relevant materials for a series of technologically important processes, such as light alkanes dehydrogenation and aromatization (Cyclar process),<sup>1</sup> hydrocarbon isomerization,<sup>2</sup> nitrogen oxides reduction by hydrocarbons,<sup>3–5</sup> and carbon dioxide hydrogenation to methanol.<sup>6–8</sup>

More recently, gallium oxide-supported metal catalysts have also proved to be active and selective for hydrogen production from the steam reforming of methanol (SRM).<sup>9,10</sup> In particular, the use of metal (Pd, Pt, or Cu) supported onto gallium oxide or gallium-modified metal oxide supports has shown a high yield of hydrogen and excellent selectivity to carbon dioxide from SRM. Iwasa et al. studied the SRM reaction on Pd and Pt supported over ZnO, In<sub>2</sub>O<sub>3</sub>, Ga<sub>2</sub>O<sub>3</sub>, SiO<sub>2</sub>, MgO, ZrO<sub>2</sub>, and CeO<sub>2</sub>, at 493 K, using a 1:1 water-to-methanol molar ratio.<sup>9</sup> They found that Ga<sub>2</sub>O<sub>3</sub>, In<sub>2</sub>O<sub>3</sub>, and ZnO gave the most active materials, with selectivity to CO<sub>2</sub> higher than 95% in all cases. Further work of Iwasa et al. using Pd-based materials confirmed that the selectivity and activity of the SRM reaction is improved by adding Zn, Cd, In, and Ga oxides to their Pd/CeO<sub>2</sub> base formulation.<sup>10</sup>

In a previous work some of us reported that methanol could be successfully synthesized on the Pd–Ga<sub>2</sub>O<sub>3</sub> system from a CO<sub>2</sub>/H<sub>2</sub> mixture (that is, the SRM reverse reaction).<sup>7</sup> Later on, Collins et al.<sup>8</sup> studied the interaction of CO<sub>2</sub> and CO<sub>2</sub>/H<sub>2</sub> on pure  $\beta$ -Ga<sub>2</sub>O<sub>3</sub> and Pd/ $\beta$ -Ga<sub>2</sub>O<sub>3</sub> by temperature-programmed

reaction experiments, between 323 and 723 K, using in situ FTIR spectroscopy. These authors proposed a bifunctional mechanism, where gaseous CO<sub>2</sub> is weakly adsorbed over the gallia surface to give carbonate and bicarbonate groups, which further react with atomic hydrogen (supplied by spillover from the Pd crystallites<sup>11</sup>) to produce mono- and dicoordinated formate. The monocoordinated formate would then hydrogenate to methoxy species. To further understand these reaction pathways, Collins et al.<sup>12</sup> examined the decomposition of methanol on Pd/ $\alpha,\beta$ -Ga<sub>2</sub>O<sub>3</sub> and Pd/SiO<sub>2</sub>, showing that gallia was indeed active to adsorb methanol, to give methoxy species that decompose to CO and CO<sub>2</sub>, whereas palladium was able to decompose methanol to HCO and CO with the simultaneous release of H<sub>2</sub>.

In terms of both the SRM and methanol synthesis, systematic study of the interaction of H<sub>2</sub>, CO<sub>2</sub>, CO, H<sub>2</sub>O, and CH<sub>3</sub>OH on pure gallium oxide seems to be a worthy effort. In situ FTIR spectroscopy studies have been performed in order to evaluate the adsorption of hydrogen (deuterium)<sup>13</sup> and carbon dioxide<sup>14</sup> over a set of  $\alpha$ -,  $\beta$ -, and  $\gamma$ -Ga<sub>2</sub>O<sub>3</sub> polymorphs. After exposing gallia samples to flowing molecular hydrogen, two infrared signals were developed at temperatures higher than 523 K, which were assigned to Ga<sup>VI</sup>–H and Ga<sup>IV</sup>–H surface bonds (where Ga<sup>VI</sup> and Ga<sup>IV</sup> stand for gallium cations in octahedral and tetrahedral coordination, respectively).<sup>13</sup> It was also found that the amount of each gallium surface site mimics the bulk coordination of  $\alpha$ -,  $\beta$ - and  $\gamma$ -gallia polymorphs. In addition, the surface basicity of the gallia surface was explored via the adsorption of carbon dioxide.<sup>14</sup> Up to six (bi)carbonate species with different thermal stability were detected by running temperature-programmed reaction experiments from 323 to 723

\* Corresponding author e-mail: aboni@intec.unl.edu.ar.

<sup>†</sup> CONICET, Universidad Nacional del Litoral.

<sup>‡</sup> CONICET, Universidad Nacional de La Plata.

**TABLE 1: Surface Area, Density of Active Sites ( $N_S$ ) for Methanol Adsorption, and Maximum Desorption Temperature ( $T_m$ ) for the Desorption Products from Activated Gallium Oxides**

sample <sup>a</sup>	$S_{\text{BET}}$ (m <sup>2</sup> g <sup>-1</sup> )	$N_S$ ( $\mu\text{mol}$ of CH <sub>3</sub> OH m <sup>-2</sup> )	$T_m$ (K)			
			CO	CO <sub>2</sub>	DME	CH <sub>3</sub> OH
$\alpha(40)$ -O	40	1.39	613	620		323–573
$\alpha(40)$ -H	40	1.04	621	621	558	323–573
$\beta(64)$ -O	64	0.97		603		323–573
$\beta(25)$ -H	25		623	640	549	331–600
$\gamma(105)$ -O	105	2.08	604	611	526	323–573
$\gamma(105)$ -H	105	1.60	600	608	508	323–573

<sup>a</sup> The samples were activated under flowing pure O<sub>2</sub> (samples coded with -O) or pure H<sub>2</sub> (samples coded with -H).

K; namely, mono- and bidentate bicarbonate, carboxylate, and bridged, bidentate, and polydentate carbonates. Except for the polydentate groups, all other species were easily removed by outgassing the samples at room temperature, thus revealing the presence of mostly weak basic sites.

The Lewis and Brønsted acidities of the  $\alpha$ -,  $\beta$ -, and  $\gamma$ - forms were also examined by FTIR, by adsorbing carbon monoxide,<sup>15–17</sup> pyridine,<sup>15,18</sup> and 2,6-dimethylpyridine.<sup>18</sup> These spectroscopic probe molecules revealed the presence of weak Brønsted acid sites and exposed that the Lewis acidity was related to coordinatively unsaturated *cus*-Ga surface ions.

Concerning the surface chemistry of the gallia polymorphs, then, all these previous investigations have shown just slight differences between the  $\alpha$ -,  $\beta$ -, and  $\gamma$ - forms. Despite this, to the best of our knowledge there is a lack of information in the open literature about the interaction between methanol and the surface of the different gallium oxide polymorphs. Therefore, we report here our results in regards to the chemisorption of methanol and its surface reactivity, via temperature-programmed surface reaction experiments followed by infrared spectroscopy and mass spectrometry, over three bulk Ga<sub>2</sub>O<sub>3</sub> polymorphs.

## 2. Experimental Section

**2.1. Materials.** All gallia polymorphs were obtained from Ga(NO<sub>3</sub>)<sub>3</sub>·*x*H<sub>2</sub>O and Ga<sub>2</sub>O<sub>3</sub> supplied by Strem Chemicals (99.99% and 99.998% Ga, respectively). We followed the basic preparation methods described in a previous work<sup>13</sup> to obtain polymorphs with Brunauer–Emmett–Teller surface area ( $S_{\text{BET}}$ ) between 12 and 105 m<sup>2</sup> g<sup>-1</sup>, as it is briefly outlined below.

Two pure phases of  $\alpha$ -Ga<sub>2</sub>O<sub>3</sub> were prepared from Ga(NO<sub>3</sub>)<sub>3</sub>·*x*H<sub>2</sub>O in aqueous NH<sub>4</sub>OH (pH = 10), at room temperature (RT). The precipitated gel was washed several times with doubly distilled water until no residual NO<sub>3</sub><sup>-</sup> anions were detected in the washing water by UV spectroscopy. One part of this gel was aged at 343 K (3 h) and dried under vacuum at 298 K (4 h), and finally, it was calcined in air at 773 K (1 h) to give  $\alpha$ -Ga<sub>2</sub>O<sub>3</sub> with a  $S_{\text{BET}}$  value of 40 m<sup>2</sup> g<sup>-1</sup> [referred to as  $\alpha(40)$ ]. Another part, which was instead calcined for 4 h, gave a  $S_{\text{BET}}$  value of 20 m<sup>2</sup> g<sup>-1</sup> [referred to as  $\alpha(20)$ ].

The  $\gamma$ - and  $\beta$ -Ga<sub>2</sub>O<sub>3</sub> phases were synthesized as follows. Hydrated gallium hydroxide gel was obtained by adding an ammonia ethanolic solution (50% v/v) to 7 wt % Ga(NO<sub>3</sub>)<sub>3</sub>·*x*H<sub>2</sub>O in ethanol at RT. The gel was filtered and washed with ethanol until no NO<sub>3</sub><sup>-</sup> anions were detected. The resulting material was then dried at 343 K (1 h) and then air calcined at 823 K (8 h). A  $\gamma$ -Ga<sub>2</sub>O<sub>3</sub> polymorph with  $S_{\text{BET}}$  value equal to 105 m<sup>2</sup> g<sup>-1</sup>, referred to as  $\gamma(105)$ , was obtained. A portion of this last gallium oxide was further calcined in air at 923 K (6 h) to give a  $\beta$ -Ga<sub>2</sub>O<sub>3</sub> ( $S_{\text{BET}}$  = 64 m<sup>2</sup> g<sup>-1</sup>), referred to as  $\beta(64)$ . Another  $\beta$ -gallia simple, referred to as  $\beta(25)$ , was prepared by direct calcination in air of the commercial gallium oxide at 1073 K during 6 h.

The crystallographic phase of each gallium oxide type was determined by X-ray diffraction spectrometry (XRD) using a Shimadzu XD-D1 apparatus (Cu K $\alpha$  radiation). The  $S_{\text{BET}}$  value of each gallium oxide, previously outgassed at 473 K for 3 h under dynamic vacuum (base pressure =  $1.33 \times 10^{-4}$  Pa), was measured at 77 K employing a Micromeritics Accusorb 2001E apparatus. The main features of the samples used in this work are summarized in Table 1.

The surface and bulk purity of the samples were evaluated by Auger electron spectroscopy (AES) and atomic absorption spectroscopy (AAS), respectively.

### 2.2. Chemisorption and Temperature-programmed Surface Reaction of Methanol. 2.2.1. Mass Spectrometry Studies.

Methanol chemisorption and temperature-programmed surface reaction experiments using mass spectrometry as a detector of the gaseous products (TPSR-MS) were performed in a microreactor coupled on-line with a mass spectrometer (Balzers QMG 112A) and a TCD (Shimadzu GC-8A). Each oxide (~10 m<sup>2</sup>) was activated at 723 K for 30 min under a flow of pure molecular oxygen (-O) or molecular hydrogen (-H) (60 cm<sup>3</sup> min<sup>-1</sup>), purged at the same temperature with He (60 cm<sup>3</sup> min<sup>-1</sup>), and cooled to 373 K (the adsorption temperature) under He flow prior to methanol chemisorption and TPSR-MS analysis. Successive pulses of 1.2  $\mu\text{mol}$  (0.5  $\mu\text{L}$ ) of methanol in a He stream were dosed onto each sample, until the surface saturation of the gallia was reached. The adsorption process was monitored in situ through a mass spectrometer and a conductivity cell to detect the nonadsorbed alcohol and/or the species desorbed from the sample. After the surface saturation, the sample was cooled from 373 to 323 K and immediately heated to 723 K at 10 K min<sup>-1</sup>, under He flow (60 cm<sup>3</sup> min<sup>-1</sup>). The following species were scanned during the TPSR-MS analysis: CH<sub>3</sub>OH (*m/e* = 31), dimethyl ether (*m/e* = 45), formaldehyde (*m/e* = 30), CO (*m/e* = 28), CO<sub>2</sub> (*m/e* = 44), H<sub>2</sub>O (*m/e* = 18), methyl formate (*m/e* = 60), formic acid (*m/e* = 46), and dimethoxy methane (*m/e* = 75).

**2.2.2. In situ Infrared Studies.** Methanol chemisorption and temperature-programmed surface reaction experiments using infrared spectroscopy as a detector of mainly surface species (TPSR-IR) were investigated by in situ transmission infrared spectroscopy on self-supporting wafers (30 mg) of each Ga<sub>2</sub>O<sub>3</sub> polymorph, pressed at 5 t cm<sup>-2</sup> (diameter = 13 mm). Each wafer was placed, in turn, into a Pyrex IR cell fitted with water-cooled NaCl windows, which was attached to a conventional high-vacuum system (base pressure =  $1.33 \times 10^{-4}$  Pa), equipped with a manifold for gas flow operation. Before the adsorption of methanol, each sample was activated into the cell, as mentioned before, either in pure O<sub>2</sub> (-O) or pure H<sub>2</sub> (-H) at 723 K for 30 min and cooled to 373 K under He flow (60 cm<sup>3</sup> min<sup>-1</sup>), to allow reference IR spectra of the “clean wafer” to be taken at different temperatures.

Methanol (Carlo Erba RPE, 99.9%) or methanol- $d_3$  (CIL-Cambridge Isotope Laboratories D, 99%) was purified by a series of freeze–thaw cycles, under vacuum, to remove dissolved gases and was stored at RT in a glass bulb attached to the manifold. Afterward, methanol vapor was allowed into a small section of the manifold (which featured a sampling loop) and then was swept from the loop by flowing He ( $60 \text{ cm}^3 \text{ min}^{-1}$ ) and admitted into the IR cell, at 373 K. After methanol adsorption onto the catalyst wafer, the cell was purged for 30 min by flowing He at  $60 \text{ cm}^3 \text{ min}^{-1}$ . Next, the temperature was decreased to 323 K. IR spectra were taken every 5 min along the process. Additional experiments using methanol- $d_3$  ( $\text{CD}_3\text{OH}$ ) and deuterated gallia samples were also performed and are described later in the text.

TPSR-IR experiments were performed over the set of methanol-adsorbed samples by heating the IR cell from 323 to 723 K at  $10 \text{ K min}^{-1}$  under He flow ( $60 \text{ cm}^3 \text{ min}^{-1}$ ). Along the temperature ramp, a transmission infrared spectrum was recorded every 25 K. A Shimadzu 8210 FT-IR spectrometer with a DLATGS detector ( $4 \text{ cm}^{-1}$  resolution, 25 scans) was used to acquire the spectra. Further processing of the data was carried out with the Microcal Origin 4.1 software. Background correction of the spectra was achieved by subtracting the spectra of the pretreated cleaned wafer at each temperature; a Lorentzian sum function was used to fit the overlapping bands and to measure peak areas and/or intensities.<sup>19</sup>

All the gases used in this study were high purity grade and were further purified as follows:  $\text{H}_2$  (AGA UHP grade 99.999%) and He (AGA UHP 99.999%) were passed through molecular sieve ( $3 \text{ \AA}$  Fisher) and  $\text{MnO}/\text{Al}_2\text{O}_3$  traps to remove water and oxygen impurities.  $\text{O}_2$  (AGA Research grade 99.996%) was passed through a molecular sieve ( $3 \text{ \AA}$  Fisher) and an Ascarite trap to remove water and  $\text{CO}_2$ . Deuterium (Scott 99.9% C.P. Grade) was introduced directly into the cell.

### 3. Results and Discussion

**3.1. Adsorption of  $\text{CH}_3\text{OH}$  ( $\text{CD}_3\text{OH}$ ) on Gallia Polymorphs at 373 K.** **3.1.1. Surface Species after Methanol Adsorption.** The adsorption of methanol on the gallia samples was carried out at 373 K in order to generate a stable monolayer of chemisorbed methoxy species. Previous studies determined that only molecular methanol is adsorbed at lower temperatures and that further surface reaction of chemisorbed species is produced at higher temperature.<sup>20–22</sup>

Upon exposing the gallia polymorphs to pulses of methanol, no gaseous oxycarbonaceous products originating from methanol oxidation or dehydration were detected, and only water, besides  $\text{CH}_3\text{OH}(\text{g})$ , evolved to the gas phase. Table 1 summarizes the density of active sites ( $N_S$ ) able to chemisorb methanol at 373 K on each gallia polymorph activated under oxygen or hydrogen. The  $N_S$  values are in the range  $1\text{--}2 \mu\text{mol m}^{-2}$  for the different crystal phases. The  $N_S$  results also indicate that the samples treated in  $\text{H}_2$  adsorbed  $\sim 25\%$  less methanol than the same samples treated in  $\text{O}_2$ .

Figure 1 shows the IR spectra collected after the adsorption of methanol at 373 K on the gallias. The position and relative intensity of the IR bands are almost identical for the different gallia crystal phases, that is, the same surface species were formed. Nevertheless, it should be noted that the intensity of the IR bands is stronger the higher the surface area of each sample is and also that for the same polymorph the hydrogen treatment reduced the intensity of the IR signals as compared to the oxygen activated samples, in agreement with the  $N_S$  results reported in Table 1.

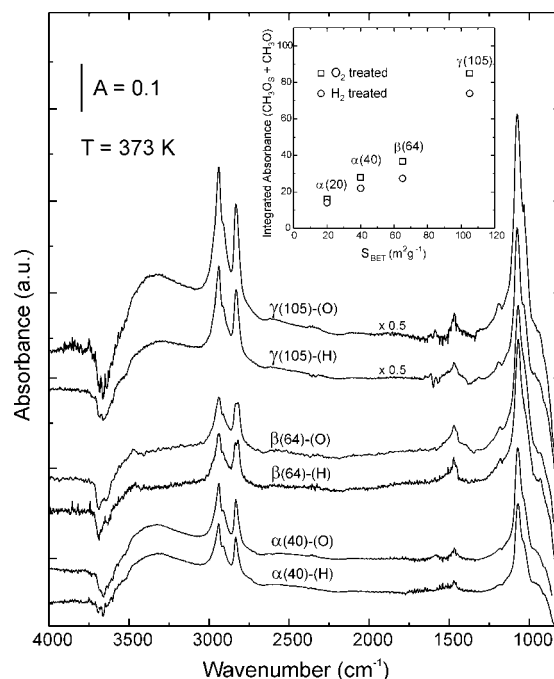


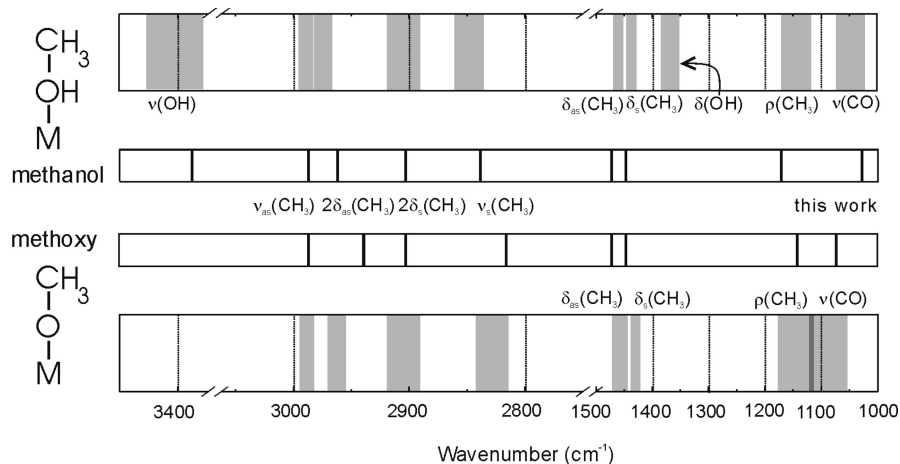
**Figure 1.** Infrared spectra after  $\text{CH}_3\text{OH}$  adsorption at 373 K on  $\alpha$ -,  $\beta$ -, and  $\gamma$ - $\text{Ga}_2\text{O}_3$  activated under oxygen (-O) or hydrogen (-H). Inset: Total integrated absorbance of  $\text{CH}_3\text{OH}_S$  [ $\nu(\text{CO}) = 1030 \text{ cm}^{-1}$ ] and  $\text{CH}_3\text{O}$  [ $\nu(\text{CO}) = 1070 \text{ cm}^{-1}$ ] species versus the surface area of the oxides.

To perform a precise assignment of the IR signals that emerged after the adsorption of  $\text{CH}_3\text{OH}(\text{g})$ , in order to distinguish between molecularly adsorbed methanol ( $\text{CH}_3\text{OH}_S$ ) and methoxy ( $\text{CH}_3\text{O}$ ), we compared the IR band positions with the spectroscopic information condensed in a correlation chart (Chart 1), which was built by compiling the IR signals of the  $\text{CH}_3\text{OH}_S$  and  $\text{CH}_3\text{O}$  species adsorbed over a wide range of metals and metal oxides reported in the literature.

Thus, it is useful to distinguish three spectral regions: (i)  $4000\text{--}3000$ , (ii)  $3000\text{--}2700$ , and (iii)  $1600\text{--}800 \text{ cm}^{-1}$ . Overlapped bands were resolved using the sum of Lorentzian curves, as is shown in Figure 2. The resulting assignment of each IR band to the corresponding vibrational mode is summarized in Table 2.

In the high-frequency range of the spectra, negative bands between  $3750$  and  $3580 \text{ cm}^{-1}$  appeared. These negative signals indicate that a perturbation or a consumption of the surface OH groups on the gallia occurred after the methanol adsorption at 373 K,<sup>13,14</sup> along with the development of a broad band between  $3500$  and  $3300 \text{ cm}^{-1}$ , which is assigned to the  $\nu(\text{OH})$  mode of molecularly adsorbed methanol. However, this last band might also have an important contribution of the  $\nu(\text{OH})$  mode of perturbed GaOH surface groups by adsorbed methanol molecules, which would produce a red shift on the original signal. To clarify this point and to confirm the assignment of the wide band, an additional adsorption experiment of  $\text{CH}_3\text{OH}$  at 373 K was performed over an  $\alpha$ - $\text{Ga}_2\text{O}_3$  sample pretreated in  $\text{D}_2$  up to 723 K, that is, where all the GaOH groups had been completely exchanged to GaOD at the surface [ $\nu(\text{OD}) = 2700\text{--}2500 \text{ cm}^{-1}$ ].<sup>14</sup> (The spectrum taken under those conditions is shown in Figure S1 of the Supporting Information). So it was proved that the bands owing to GaOD species were consumed (no shift was observed) after the methanol adsorption at 373 K, whereas the broad signal at  $>3000 \text{ cm}^{-1}$  still was present in the spectrum. These results indicate that the hydroxyl groups on the gallia



**CHART 1: Infrared vibrational frequency correlation chart of adsorbed methanol ( $\text{CH}_3\text{OH}_s$ ) and methoxy ( $\text{CH}_3\text{O}$ ) species over several metals or metal oxides**


surface react with methanol to give methoxy species and water gas molecules, as observed by mass spectrometry (MS). Therefore, the broad band centered at  $\sim 3300\text{ cm}^{-1}$  can be clearly attributed to the  $\nu(\text{OH})$  mode of molecularly adsorbed methanol ( $\text{CH}_3\text{OH}_s$ ). This band is red-shifted by almost  $200\text{ cm}^{-1}$  with respect to the  $\nu(\text{OH})$  of the free methanol molecule, which indicates the presence of a relatively strong hydrogen-bridge bond between the  $\text{CH}_3\text{OH}_s$  and the basic  $\text{O}^{2-}$  sites on the gallia surface.<sup>23,24</sup>

The IR spectra in the C–H stretching region ( $3000\text{--}2700\text{ cm}^{-1}$ ) show a set of overlapped bands (see Figure 2) whose assignment presents some controversy in the literature. Some authors, particularly those working on the field of heterogeneous catalysis, have attributed the most intense couple of peaks (that is, the ones centered at  $\sim 2950$  and  $\sim 2850\text{ cm}^{-1}$ ) to the asymmetric and symmetric stretching modes of methoxy groups [ $\nu_{\text{as}}(\text{CH}_3)$  and  $\nu_{\text{s}}(\text{CH}_3)$ , respectively] bonded to either the support or the metal particles.<sup>25–29</sup>

However, different assignments have also been reported for the same set of IR bands of methyl groups attached to a variety of polar and/or unsaturated groups, as well as to some metal oxide surfaces. For instance, Derouault et al.<sup>30</sup> and Lavalley and Sheppard<sup>31</sup> attributed these overlapped bands, at increasing wavenumbers, to the following modes: the overtone of the symmetric C–H bending vibration [ $2\delta_{\text{s}}(\text{CH}_3)$ ] at  $2750\text{--}2850\text{ cm}^{-1}$ , the overtone of the asymmetric C–H bending vibration [ $2\delta_{\text{as}}(\text{CH}_3)$ ] at  $2890\text{--}2910\text{ cm}^{-1}$ , the  $\nu_{\text{s}}(\text{CH}_3)$  at  $\sim 2960\text{--}2900\text{ cm}^{-1}$ , and the  $\nu_{\text{as}}(\text{CH}_3)$  at  $>2950\text{ cm}^{-1}$ . To sustain their

assignments, these last authors performed a systematic analysis of the anharmonicity parameters and Fermi resonance contributions of those vibrational modes in a large diversity of  $\text{CH}_3\text{-X}$  molecules (where X stands for Cl, Br, I,  $\text{SnCl}_3$ ,  $\text{SiCl}_3$ ,  $\text{SCN}$ ,  $\text{COC}_6\text{H}_5$ ,  $\text{CN}$ ,  $\text{CH}_2\text{Br}$ ,  $\text{C}_6\text{H}_5$ ,  $\text{NCS}$ ,  $\text{NCO}$ ,  $\text{OOC}$ , etc.).<sup>31</sup> Similar assignment sequence was previously reported for methyl bonded to aromatic rings and to polar groups (e.g.,  $\text{CCl}_3\text{COO}$ ,  $\text{N}(\text{CH}_3)_2$ ,  $\text{N-Aryl}$ , etc.).<sup>32</sup> So, several authors have recently used the preceding approach to assign the IR bands in the  $3000\text{--}2700\text{ cm}^{-1}$  region to methanol and/or methoxy bonded to the surface of different powdered metal oxides mostly used as catalysts or catalyst supports.<sup>12,23,24,33–38</sup>

From the point of view of surface science, vibrational studies of methoxy and methanol adsorbed over the surface of single crystals—based on the use of labeled molecules, ab initio calculations, and group theory—have led us to conclude that the signals in this high-frequency region should be assigned, again at ascending wavenumbers, to (i) the  $\nu_{\text{s}}(\text{CH}_3)$  mode, (ii) the  $2\delta_{\text{s}}(\text{CH}_3)$  and  $2\delta_{\text{as}}(\text{CH}_3)$  overtones [both having enhanced intensities due to Fermi resonance with the  $\nu_{\text{s}}(\text{CH}_3)$  mode], and (iii) the  $\nu_{\text{as}}(\text{CH}_3)$  mode (which is active in IR for methoxy species with  $\text{C}_s$  symmetry or lower).<sup>39–48</sup> This assignment sequence is in agreement with the earliest vibrational studies of methanol and related molecules (e.g.,  $\text{CH}_3$  groups attached to an aromatic ring, halides, methylhalides, or  $\text{CN}$ ) in liquid or gaseous phases and also in solid matrixes.<sup>49–51</sup>

Clearly, further experimental and theoretical work will be necessary to solve the controversy on the band assignment for adsorbed methanol and/or methoxy in the  $3000\text{--}2700\text{ cm}^{-1}$  IR region, using single crystal planes of different metal oxides. However, at this point, we think that the last approach is more sound.

Accordingly, as indicated in Figure 2, the nondissociated adsorbed methanol is characterized by the  $\nu_{\text{s}}(\text{CH}_3)$  and  $2\delta_{\text{s}}(\text{CH}_3)$  couple at slightly higher frequencies than those of methoxy groups.<sup>34,39</sup> The very weak band (shoulder) at  $2990\text{ cm}^{-1}$  is attributed to the  $\nu_{\text{as}}(\text{CH}_3)$  in both the  $\text{CH}_3\text{OH}_s$  and  $\text{CH}_3\text{O}$  species, which might be IR active due to their tilted geometry—loss of the  $\text{C}_{3v}$  symmetry—as described by DFT calculations on  $\beta\text{-Ga}_2\text{O}_3(100)$ .<sup>24</sup> The peak centered at  $2960\text{ cm}^{-1}$  is the result of two superimposed signals at  $2958$  and  $2940\text{ cm}^{-1}$  assigned to the first overtone of the C–H asymmetric deformation mode,  $2\delta_{\text{as}}(\text{CH}_3)$  of the  $\text{CH}_3\text{OH}_s$  and  $\text{CH}_3\text{O}$  surface species, respectively. The signal at  $2907\text{ cm}^{-1}$  corresponds to the  $2\delta_{\text{s}}(\text{CH}_3)$  of

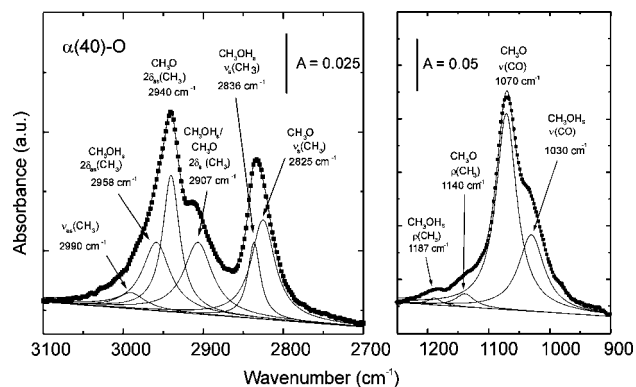


**Figure 2.** Resolved IR signals for the IR modes of  $\text{CH}_3\text{OH}_s$  and  $\text{CH}_3\text{O}$  surface species.

**TABLE 2: Infrared Bands Assignment to Methanol and Methoxy Groups Adsorbed over the Gallia Polymorphs<sup>a</sup>**

IR mode	wavenumber (cm <sup>-1</sup> )		
	CH <sub>3</sub> OH(g)	CH <sub>3</sub> OH <sub>S</sub> on Ga <sub>2</sub> O <sub>3</sub>	CH <sub>3</sub> O- on Ga <sub>2</sub> O <sub>3</sub>
$\nu(\text{OH})$	3709(R) 3681(Q) 3664(P)	3550–3000	
$\nu_{\text{as}}(\text{CH}_3)$	3006 2973		2997
$\nu_{\text{s}}(\text{CH}_3)^b$	2868(R) 2844(Q) 2826(P)	2958	2940
2 $\delta_{\text{as}}(\text{CH}_3)^b$			2907
2 $\delta_{\text{s}}(\text{CH}_3)^b$			2836
$\delta_{\text{as}}(\text{CH}_3)$	1474		1510
$\delta_{\text{s}}(\text{CH}_3)$	1453		1469
$\delta(\text{OH})$	1345	n.d. <sup>c</sup>	
$\rho(\text{CH}_3)$		1183	1126
$\nu(\text{CO})$	1057(R) 1032(Q) 1014(P)	1030	1070

<sup>a</sup> Average experimental values. <sup>b</sup> Strongly perturbed by Fermi resonance. <sup>c</sup> Not detected.

both species. Finally, the C–H symmetric stretching [ $\nu_{\text{s}}(\text{CH}_3)$ ] mode can be resolved into individual bands at 2836 and 2825 cm<sup>-1</sup> for the molecularly adsorbed methanol and for the methoxy groups, respectively.

In addition, an extra experiment was performed by exposing the  $\alpha$ -Ga<sub>2</sub>O<sub>3</sub> sample to methanol-*d*<sub>3</sub> at 373 K, which confirmed the previous mode assignments. Infrared bands of the CD<sub>3</sub>OH<sub>S</sub> and CD<sub>3</sub>O species were detected and assigned as shown in Table 3 (see also the TPSR-IR section below). The experimental value for the ratio between the stretching frequencies of C–H and C–D bonds was 1.37, which is fairly close to the expected value (1.36) for the  $\nu(\text{C–H})$  versus the  $\nu(\text{C–D})$  symmetric or asymmetric modes. The C–D deformation modes and their overtones were further assigned according to literature data, based on the spectra of the CD<sub>3</sub>OH monomer in CCl<sub>4</sub> solution,<sup>23</sup> CD<sub>3</sub>OD in an Ar matrix,<sup>44</sup> CD<sub>3</sub>OH adsorbed on  $\delta$ -Al<sub>2</sub>O<sub>3</sub>,<sup>23</sup> and CD<sub>3</sub>O species on metal surfaces (Ag,<sup>44</sup> Rh,<sup>45</sup> and Cu<sup>43</sup>). It should be also noted that no isotopic scrambling was produced between the CD<sub>3</sub>OH molecule and the gallia surface at this temperature.

All in all it seems that, whichever the precise assignment that could be made of each of the spectral features in the 3000–2700 cm<sup>-1</sup> region, such bands are not appropriate to follow the thermal evolution of molecularly adsorbed methanol and methoxy groups due to the high overlapping of the several modes of both species, which is better achieved using the low frequency bands, basically the C–O stretching vibration, as it is shown below.

In the low wavenumber region the asymmetric and symmetric bending C–H modes of both CH<sub>3</sub>OH<sub>S</sub> and CH<sub>3</sub>O groups were observed at 1469 [ $\delta_{\text{as}}(\text{CH}_3)$ ] and 1451 cm<sup>-1</sup> [ $\delta_{\text{s}}(\text{CH}_3)$ ], respectively. The IR signals of the C–H rocking modes [ $\rho(\text{CH}_3)$ ] of methanol and methoxy groups could be discerned at 1183 and 1126 cm<sup>-1</sup>, but with low intensity. In this spectral region the very strong C–O stretching vibration [ $\nu(\text{CO})$ ] allows a straightforward distinction between CH<sub>3</sub>OH<sub>S</sub> and CH<sub>3</sub>O because, typically, the molecularly adsorbed methanol exhibits a  $\nu(\text{CO})$  signal close to the one of the gas phase molecule [ $\nu(\text{CO}) = 1032$  cm<sup>-1</sup>], whereas the same mode is shifted to higher frequencies in the methoxy species. These strong bands at 1070 and 1030 cm<sup>-1</sup>, attributed to CH<sub>3</sub>O and CH<sub>3</sub>OH<sub>S</sub> surface species, respectively, are therefore useful to follow the evolution

of their surface concentration throughout the TPSR-IR experiments. Lastly, to complete the interpretation of the IR spectral features, it is possible to explain the negative band at 820 cm<sup>-1</sup> on all the samples as due to a perturbation of the Ga–O surface mode, in similar fashion to the results reported by Busca et al. where methanol was adsorbed on  $\delta$ -alumina.<sup>23</sup>

At this point we can conclude that, after exposing the Ga<sub>2</sub>O<sub>3</sub> surface to methanol at 373 K, two spectroscopically different surface species are produced, irrespective of the gallia polymorph and the activation procedure (under O<sub>2</sub> or H<sub>2</sub>): (i) molecularly adsorbed, Lewis-bound, methanol (CH<sub>3</sub>OH<sub>S</sub>) and (ii) dissociatively adsorbed methoxy groups (CH<sub>3</sub>O).<sup>23,34–38,52</sup>

Methanol adsorption has also been employed as an IR probe molecule to characterize the redox behavior of reducible metal oxides. For example, it made possible the differentiation of the oxidation state and coordination of Ce<sup>3+</sup> and Ce<sup>4+</sup> cations sites on the surface of ceria and ceria-zirconia, due to a shift of the  $\nu(\text{CO})$  mode.<sup>53–56</sup> In our case, some of us have earlier proved that the surface of gallium oxide can be partially reduced upon hydrogen treatment at 723 K.<sup>13,57</sup> Notwithstanding, after investigating the chemisorption of methanol over a wide diversity of gallia polymorphs (which involves different Ga surface sites, namely, Ga<sup>IV</sup> and Ga<sup>VI</sup>), treated under oxygen or hydrogen, no direct spectroscopic identification of those different Ga sites could be done here.

Nevertheless, we can still put forth some extra effort and search for clues about the coordination of the methoxy groups bonded to the gallia surface. Lamotte et al.<sup>58</sup> postulated that the position of the  $\nu(\text{CO})$  band is sensitive to the coordination of the CH<sub>3</sub>O groups bonded onto the surface of ThO<sub>2</sub> and CeO<sub>2</sub>, in the following order: mono- [ $\nu(\text{CO}) = 1124$ – $1104$  cm<sup>-1</sup>], di- [ $\nu(\text{CO}) = 1061$ – $1057$  cm<sup>-1</sup>], and tricoordinated methoxy [ $\nu(\text{CO}) = 1013$  cm<sup>-1</sup>]. Similarly, Ouyang et al.<sup>59</sup> assigned IR bands at 1150 and 1050 cm<sup>-1</sup> to terminal (monocoordinated) and bridged (dicoordinated) methoxy on ZrO<sub>2</sub>, respectively. Unfortunately, methanol adsorption at 373 K on gallium oxides yielded only one IR band corresponding to the CH<sub>3</sub>O species, at 1070 cm<sup>-1</sup>; consequently, it was not possible to establish its surface coordination from the position of the  $\nu(\text{CO})$  signal. However, it is possible to explore another resource; it has also been proposed that the surface coordination of methoxy groups can be determined according to their reactivity. In this regard, Lamotte et al.<sup>58</sup> showed that the ability of surface methoxy to react with CO<sub>2</sub> to produce surface methylcarbonate groups [CH<sub>3</sub>O(CO<sub>3</sub>)] depends on the surface coordination of the CH<sub>3</sub>O species. The first step in this reaction is an electron donor–acceptor interaction between the lone pairs of the methoxy oxygen and the carbon atom of CO<sub>2</sub>. Such interaction is possible in the case of monocoordinated CH<sub>3</sub>O species, is more difficult for the dicoordinated, and is practically impossible for the tricoordinated one.

Therefore, the interaction between methoxy species adsorbed on gallia and CO<sub>2</sub> was further addressed. After adsorbing methanol at 373 K on  $\beta(64)$ -O to form CH<sub>3</sub>O and CH<sub>3</sub>OH<sub>S</sub>, any remaining physisorbed and/or gaseous methanol was removed by flowing He, as previously described. Then, the IR cell was cooled to 298 K, and CO<sub>2</sub> (760 Torr) was admitted into the cell. Almost immediately, strong bands emerged at 1595, 1467, and 1366 cm<sup>-1</sup>, together with two weak peaks at 1197 and 1109 cm<sup>-1</sup>, all of which are typical of methylcarbonate species.<sup>58,60,61</sup> Furthermore, the intensity of the 1070 cm<sup>-1</sup> signal (corresponding to CH<sub>3</sub>O) decreased by  $\sim 30\%$  from its original value, whereas the 1030 cm<sup>-1</sup> band (corresponding to CH<sub>3</sub>OH<sub>S</sub> groups) become barely smaller ( $\sim 2\%$ ). This result cleanly shows

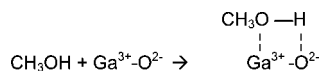
TABLE 3: Infrared Bands Assignment to CD<sub>3</sub>OH<sub>s</sub> and CD<sub>3</sub>O Groups Adsorbed over  $\alpha$ -Gallia and Model Systems

vibrational mode	wavenumber (cm <sup>-1</sup> )							
	CD <sub>3</sub> OD in Ar matrix <sup>44</sup>	CD <sub>3</sub> OH in CCl <sub>4</sub> <sup>23</sup>	CD <sub>3</sub> OH <sub>s</sub> on $\delta$ -Al <sub>2</sub> O <sub>3</sub> <sup>23</sup>	CD <sub>3</sub> O on Cu <sup>43</sup>	CD <sub>3</sub> O on Ag <sup>44</sup>	CD <sub>3</sub> O on Rh <sup>45</sup>	CD <sub>3</sub> OH <sub>s</sub> on Ga <sub>2</sub> O <sub>3</sub> <sup>d</sup>	CD <sub>3</sub> O on Ga <sub>2</sub> O <sub>3</sub> <sup>d</sup>
$\nu$ (OH)	2705 $\nu$ (OD)	3645	3200				3500–3000	
2 $\delta$ (OH)			2700				2734	
$\nu_{as}$ (CD <sub>3</sub> )	2254/2218	2230/2210	2230/2210		2209	2247		2257
$\nu_s$ (CD <sub>3</sub> ) <sup>b</sup>	2078	2070	2080–2260	2053	2064	2073/2064	2071	2060
2 $\delta_s$ (CD <sub>3</sub> ) <sup>b</sup>	2266			2172	2240	2216/2228 <sup>c</sup>	2222	2197
$\delta$ (OH)	776 $\delta$ (OD)	1293	1420					
2 $\delta_{as}$ (CD <sub>3</sub> ) <sup>b</sup>	2132	2134	2140	2112				2135
$\delta_s$ (CD <sub>3</sub> ) <sup>b</sup>	1133	1119	1130	1104 <sup>c</sup>	1120	1119		1110
$\delta_{as}$ (CD <sub>3</sub> ) <sup>b</sup>	1081/1068	1064		1081 <sup>c</sup>	1086/1064	1096/1111		1027
$\rho$ (CH <sub>3</sub> )	1032/895				895			
$\nu$ (CO)	983	978	1060–980	971	976	978/966/941	903	958

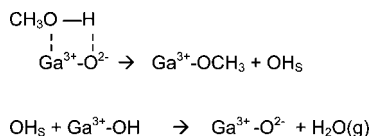
<sup>a</sup> This work. <sup>b</sup> Strongly perturbed by Fermi resonance. <sup>c</sup> Ab initio calculations.

the very fast reaction between CO<sub>2</sub> and the CH<sub>3</sub>O surface groups on Ga<sub>2</sub>O<sub>3</sub> at room temperature and suggests that methoxy species are mainly monocoordinated to the surface of gallia (see Figure S2 in the Supporting Information).

**3.1.2. Mechanistic and Quantitative Aspects of the Methanol Adsorption.** The weak perturbation in the  $\nu$ (CO) mode, at 1030 cm<sup>-1</sup>, and the large shift to lower wavenumbers of the  $\nu$ (OH) mode of CH<sub>3</sub>OH<sub>s</sub> in comparison with the monomeric (or isolated) methanol molecule (Table 2) point to a relatively strong interaction between the OH group of CH<sub>3</sub>OH and an acid–basic pair of the solid surface (Ga<sup>3+</sup>–O<sup>2-</sup>), similar to the type-II species reported by Busca et al. over  $\delta$ -Al<sub>2</sub>O<sub>3</sub>,<sup>23</sup> as described by the following reaction:



The generation of CH<sub>3</sub>O surface groups involves the breakage of the O–H bond of the methanol molecule and, subsequently, the reaction of the subtracted H with a neighbor Ga–OH group of the gallia surface, which releases a water molecule to the gas phase, as shown by mass spectrometry during the adsorption process. These two reaction steps can be drawn as follows:



Thus, the formation of methoxy groups could proceed according to a Langmuir–Hinshelwood mechanism. However, the Eley–Rideal reaction pathway can also explain the present experimental results; gaseous CH<sub>3</sub>OH would then react straightforwardly with Ga<sup>3+</sup>–OH groups to provide the CH<sub>3</sub>O species and water. Which mechanism prevails, or proceeds, is beyond the scope of the present work, but future efforts are being addressed to discern between those options.

It was further noticed by IR spectroscopy that the total amount of CH<sub>3</sub>OH<sub>s</sub> and CH<sub>3</sub>O increases as the S<sub>BET</sub> of the gallia samples does (see inset in Figure 1). However, the  $\gamma$ -polymorph shows a much higher capacity for methanol adsorption than the other samples. This trend was also exhibited upon measuring the N<sub>S</sub> of methanol by MS (Table 1). The increase in N<sub>S</sub> from  $\sim 1 \mu\text{mol m}^{-2}$  for the  $\alpha$ - and  $\beta$ -Ga<sub>2</sub>O<sub>3</sub> to  $\sim 2 \mu\text{mol m}^{-2}$   $\gamma$ -Ga<sub>2</sub>O<sub>3</sub> could probably be a consequence of the higher surface area and/or

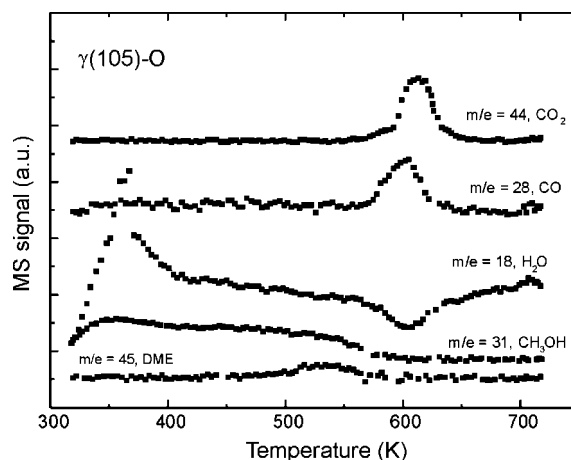


Figure 3. TPSR followed by mass spectrometry between 323 and 723 K after the adsorption of methanol at 373 K on a  $\gamma$ (105)-O sample (heating rate = 10 K min<sup>-1</sup>, 60 cm<sup>3</sup> He min<sup>-1</sup>).

lower crystallinity of the  $\gamma$ -Ga<sub>2</sub>O<sub>3</sub> sample as compared with the other polymorphs. Thus, a greater concentration of defect sites and/or different types of sites (that is, a change in the relative concentration of acid–base sites for methanol adsorption) might be used as an explanation of this “anomalous” increase in the total concentration of the adsorbed species on  $\gamma$ -Ga<sub>2</sub>O<sub>3</sub>.

Another point of concern is the lower capacity of methanol adsorption for the oxides activated under H<sub>2</sub> as compared to the ones under O<sub>2</sub> (see inset in Figure 1 and Table 1). The  $\sim 25\%$  decrease in the N<sub>S</sub> is close to the  $\sim 28\%$  of the reduction of Ga<sup>3+</sup> cations to Ga <sup>$\delta$</sup>  (  $\delta < 2$ ), as reported on Ga<sub>2</sub>O<sub>3</sub> supported on silica.<sup>57</sup> So, the partial transformation of Ga<sup>3+</sup>–O<sup>2-</sup> into Ga <sup>$\delta$</sup> –O<sup>2-</sup> sites might reduce the strength of the CH<sub>3</sub>OH–Ga interaction and, presumably, the ability to form CH<sub>3</sub>O species. Hence, an inferior amount of adsorbed methanol was expected on the partially reduced gallia.

**3.2. Temperature-programmed Surface Reaction of Adsorbed CH<sub>3</sub>OH and CH<sub>3</sub>O Groups.** **3.2.1. TPSR of Adsorbed Methanol.** Mass spectrometry (MS) results revealed the appearance of several oxycarbonaceous species in the gas phase—methanol, dimethyl ether, carbon monoxide, and carbon dioxide—along the entire range of the TPSR–MS experiments for the various oxygen or hydrogen pretreated gallias (see for example Figures 3 and 4, and Supporting Information). Methanol ( $m/e = 31$ ) desorbed in a broad band, from 323 to 573 K, exhibiting a maximum at 360–390 K for the different polymorphs. The desorption at low temperature ( $T < 423$  K) is



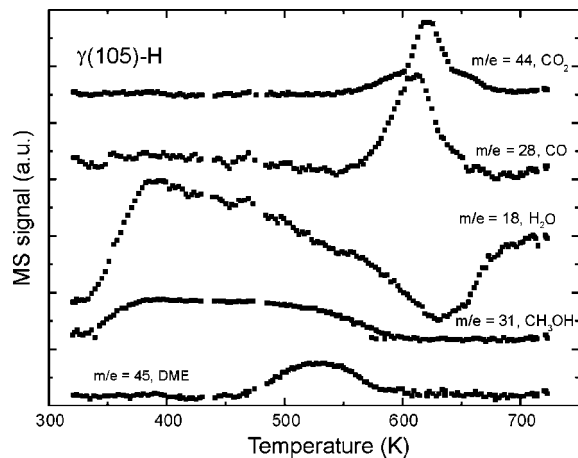


**Figure 4.** TPSR followed by mass spectrometry between 323 and 723 K after the adsorption of methanol at 373 K on a  $\gamma(105)$ -H sample (heating rate = 10 K min<sup>-1</sup>, 60 cm<sup>3</sup> He min<sup>-1</sup>).

mainly due to molecularly adsorbed methanol, whereas the high-temperature tail of the CH<sub>3</sub>OH trace can be attributed to the rehydrogenation of methoxy species by hydroxyl groups.<sup>21</sup> Water ( $m/e = 18$ ) evolves throughout the temperature ramp, showing a peak at around 350–400 K due to the desorption of molecular H<sub>2</sub>O generated during the methanol adsorption, which still remained adsorbed below such temperature. The high-temperature part of the water release can be ascribed to the dehydration of the gallium oxide. Also, it is worth mentioning that a consumption of water was registered between 573 and 673 K. The evolution of dimethyl ether ( $m/e = 45$ ), detected in the range of 473–573 K, is due to the reaction between methanol and methoxy species on surface acidic sites.<sup>21</sup> Finally, the release of oxidation products was detected at higher temperature: carbon monoxide ( $m/e = 28$ ) at ~600 K and carbon dioxide ( $m/e = 44$ ) at ~620 K. Interestingly, the production of H<sub>2</sub>CO, usually associated to the presence of redox sites on oxides, could not be discriminated from the background signal in any of the studied polymorphs.<sup>21</sup> Table 1 summarizes the TPSR-MS results for the whole set of pretreated gallias, including the nature of the desorbed species and the characteristic surface reaction temperatures.

The thermal evolution of the adsorbed species on the gallium oxides surface was followed by temperature-programmed surface reaction experiments monitored by in situ IR spectroscopy (TPSR-IR). Figures 5–7 show the IR spectra during the TPSR-IR on the oxygen-activated  $\alpha$ -,  $\beta$ -, and  $\gamma$ -Ga<sub>2</sub>O<sub>3</sub> polymorphs, respectively, between 332 and 723 K (the TPSR-IR results corresponding to the hydrogen activated gallias are presented in the Supporting Information section). The most appropriate IR signal for each identified surface species was used to follow the thermal evolution of their integrated absorbance (that is, surface concentration), as shown in Figures 8–10 for the oxygen activated gallia samples.

The TPSR-IR results show that the concentration of CH<sub>3</sub>OH<sub>s</sub> species decreased steadily, from 323 K onward, to vanish at 500 K. The concentration of CH<sub>3</sub>O groups grew slightly at first ( $T < 423$  K) but then diminished, finally disappearing at 623 K. From 473 K upward, that is, from the pronounced consumption of methoxy groups, several peaks emerged in the 1650–1300 cm<sup>-1</sup> region. The position and relative intensity of this set of bands refers to formate groups with different surface coordination, as it has been reported over a diversity of metal oxides and organometallic complexes. According to Busca and Lorenzelli,<sup>62</sup> formate species can be distinguished from each other

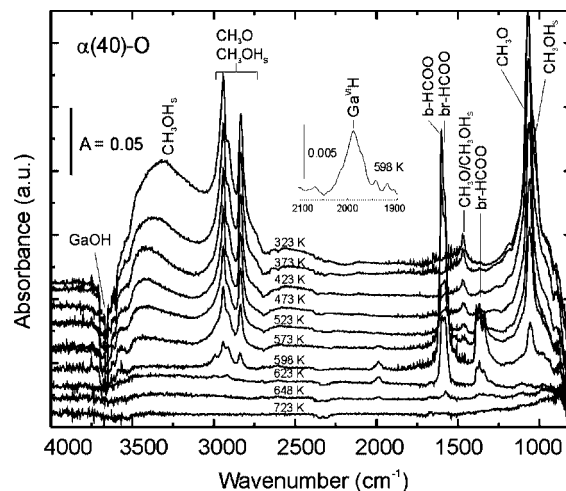


**Figure 5.** Infrared spectra during the TPSR of adsorbed CH<sub>3</sub>OH at 373 K on  $\alpha(40)$ -O (heating rate = 10 K min<sup>-1</sup>, 60 cm<sup>3</sup> He min<sup>-1</sup>).

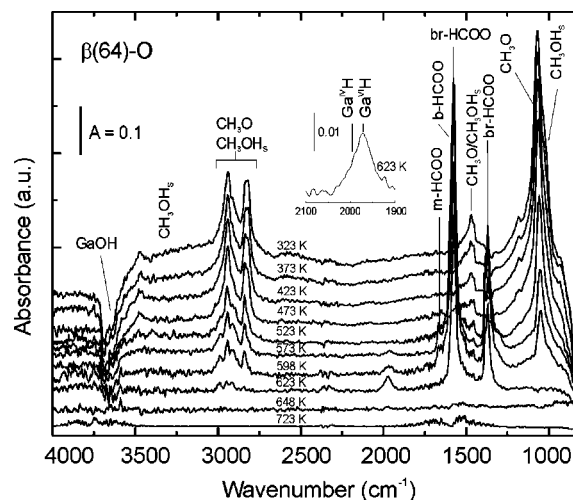


**Figure 6.** Infrared spectra during the TPSR of adsorbed CH<sub>3</sub>OH at 373 K on  $\beta(64)$ -O (heating rate = 10 K min<sup>-1</sup>, 60 cm<sup>3</sup> He min<sup>-1</sup>).

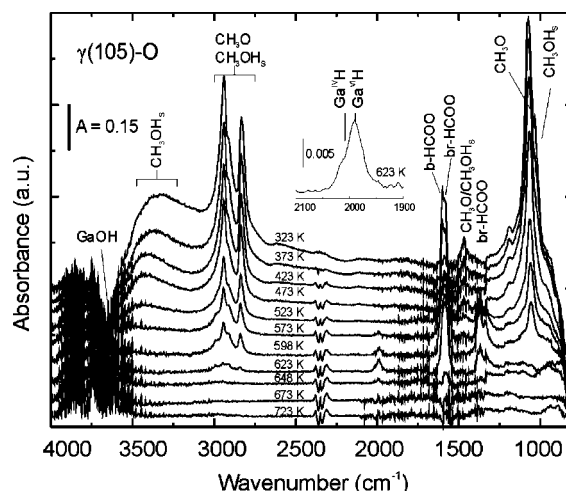


**Figure 7.** Infrared spectra during the TPSR of adsorbed CH<sub>3</sub>OH at 373 K on  $\gamma(105)$ -O (heating rate = 10 K min<sup>-1</sup>, 60 cm<sup>3</sup> He min<sup>-1</sup>).

by the band-splitting of the asymmetric and symmetric OCO stretching modes [ $\Delta\nu(\text{OCO}) = \nu_{\text{as}}(\text{OCO}) - \nu_{\text{s}}(\text{OCO})$ ]. After comparing the wavenumber location of the  $\nu_{\text{as}}(\text{OCO})$  and  $\nu_{\text{s}}(\text{OCO})$  of formate metallic complexes whose structures were determined by X-ray diffraction, it was possible to conclude

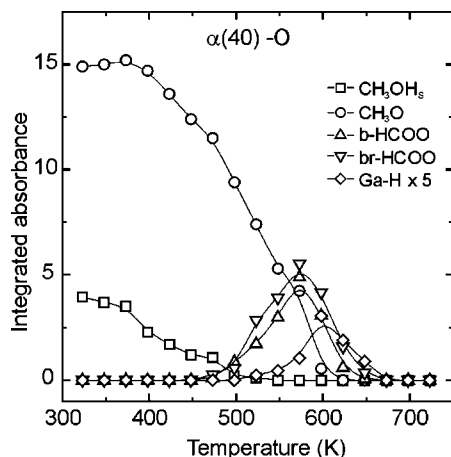


**Figure 8.** Evolution of the intensity of the infrared bands of the surface species on the  $\alpha(40)$ -H sample during the TPSR-IR:  $\text{CH}_3\text{OH}_5$  [ $\nu(\text{CO}) = 1030 \text{ cm}^{-1}$ ],  $\text{CH}_3\text{O}$  [ $\nu(\text{CO}) = 1070 \text{ cm}^{-1}$ ], b-HCOO [ $\nu_{\text{as}}(\text{OCO}) = 1600 \text{ cm}^{-1}$ ], br-HCOO [ $\nu_{\text{as}}(\text{OCO}) = 1580 \text{ cm}^{-1}$ ], and Ga-H [ $\nu(\text{Ga-H}) = 1990 \text{ cm}^{-1}$ ].

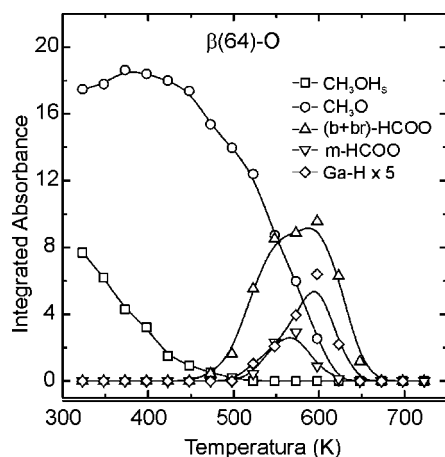


**Figure 9.** Evolution of the intensity of the infrared bands of the surface species on the  $\beta(64)$ -H sample during the TPSR-IR. Bands assignment as in Figure 8.

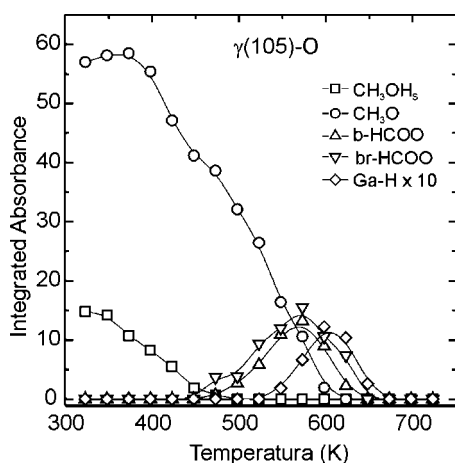


**Figure 10.** Evolution of the intensity of the infrared bands of the surface species on the  $\gamma(105)$ -H sample during the TPSR-IR. Bands assignment as in Figure 8.

the following  $\Delta\nu(\text{OCO})$  progression for the monodentate, bidentate, and bridged formate species: m-HCOO > b-HCOO  $\geq$  br-HCOO, respectively.<sup>34,54,62–67</sup> However, the positions of the  $\nu_{\text{as}}(\text{OCO})$  and  $\nu_{\text{s}}(\text{OCO})$  bands for bidentate- and bridged-formate are very close, and a distinction between these two

**TABLE 4: Infrared Signals of Formate Groups Adsorbed on the Gallia Polymorphs**

species	vibrational mode	$\nu_{\text{H}}$ ( $\text{cm}^{-1}$ )	$\nu_{\text{D}}$ ( $\text{cm}^{-1}$ )
		HCOO	DCOO
m-HCOO	$\nu(\text{OCO}) + \delta(\text{CH/D})$	nd <sup>a</sup>	nd
	$\nu(\text{CH/D})$	2910	nd
	$\nu_{\text{as}}(\text{OCO})$	1665	nd
	$\delta(\text{CH/D})$	nd	nd
	$\nu_{\text{s}}(\text{OCO})$	1305	nd
	$\Delta\nu(\text{OCO})$	360	
b-HCOO	$\nu(\text{OCO}) + \delta(\text{CH/D})$	2992	nd
	$\nu(\text{CH/D})$	2895	nd
	$\nu_{\text{as}}(\text{OCO})$	1600	1593
	$\delta(\text{CH/D})$	1355	nd
	$\nu_{\text{s}}(\text{OCO})$	1332	1316
	$\Delta\nu(\text{OCO})$	268	277
br-HCOO	$\nu(\text{OCO}) + \delta(\text{CH/D})$	2992	nd
	$\nu(\text{CH/D})$	2915	2215
	$\nu_{\text{as}}(\text{OCO})$	1580	1575
	$\delta(\text{CH/D})$	1385	nd
	$\nu_{\text{s}}(\text{OCO})$	1369	1339
	$\Delta\nu(\text{OCO})$	211	236

<sup>a</sup> Not detected.

species is difficult from experimental data alone. In the past, some of us have assigned the bands at 1580 and 1372  $\text{cm}^{-1}$  to b-HCOO species. Nevertheless, recent theoretical results allow us to reassign these bands to the more stable bridged formate groups. Thus, the stability of several formate groups on the  $\beta$ - $\text{Ga}_2\text{O}_3$  (100) surface was studied using periodic density functional theory (DFT) after the reaction of carbon monoxide with OH surface species.<sup>68</sup> It is now possible to propose that the best assignment of the IR signals for m-HCOO, b-HCOO, and br-HCOO species on gallia is the one presented in Table 4 (this was further confirmed in a deuterium-labeled experiment, as discussed below). For high concentrations of these surface formate species, the CH stretching vibration [ $\nu(\text{CH})$ ] located at 2895/2910  $\text{cm}^{-1}$  and the combination band [ $\nu_{\text{comb}} = \nu_{\text{as}}(\text{OCO}) + \delta(\text{CH})$ ] at 2991  $\text{cm}^{-1}$  could also be registered.

Together with the thermal evolution of the formate IR signals, a couple of convoluted IR bands were detected around 2003–1990  $\text{cm}^{-1}$  from 573 K; they correspond to Ga–H species on the gallia surface.<sup>8,13</sup> It is possible to distinguish, in the insets in Figures 5–7, between the  $\text{Ga}^{\text{IV}}\text{–H}$  and  $\text{Ga}^{\text{VI}}\text{–H}$  vibration modes corresponding to gallium cations in tetrahedral and octahedral positions, respectively.<sup>13</sup> The surface coverage of these Ga–H species reaches a maximum value at 600 K and sharply decays above 623 K (Figures 8–10).

Another pair of IR bands showed up in the CH stretching region of the IR spectra recorded above 573 K. These signals, located at 2948 and 2845  $\text{cm}^{-1}$ , are assigned to methylenbisoxo ( $\text{H}_2\text{COO}$ ) species, as follows.

Figure 11 displays two of the spectra taken during the TPSR-IR experiment over the oxygen activated  $\gamma$ - $\text{Ga}_2\text{O}_3$  sample at different temperatures: spectrum A, taken at 473 K, shows that only  $\text{CH}_3\text{O}$  species are present (because at such temperature  $\text{CH}_3\text{OH}_5$  has been already eliminated from the surface) and, at the same time, they are not yet further decomposed to formate groups. Spectrum B, taken at 623 K, instead depicts that methoxy species are no longer observed (note that the stronger peak at 1070  $\text{cm}^{-1}$  is not present). Finally, for comparison purposes, a third spectrum is also included in Figure 11. This last spectrum was registered after the reactive adsorption of pure CO (0.1 MPa) at 623 K. Here only HCOO species are present on the gallia surface, due to the reaction of CO with the GaOH groups ( $\text{CO} + \text{OH} \rightarrow \text{HCOO}$ ).<sup>69</sup>



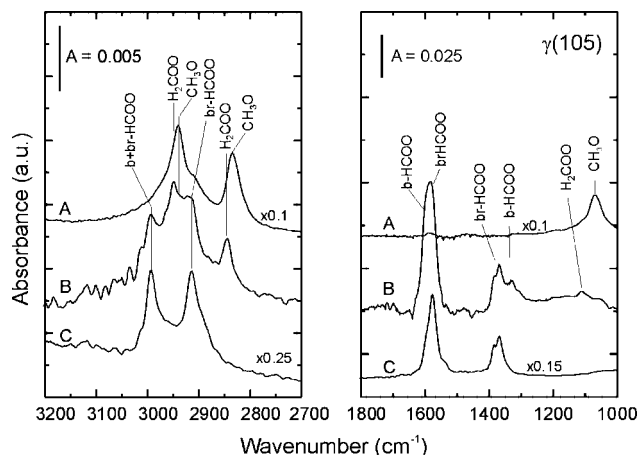


**Figure 11.** Infrared spectra acquired during the TPSR of adsorbed methanol/methoxy species, at 473 K (A) and 623 K (B). Spectrum C was taken at 623 K after the adsorption of pure CO (0.1 MPa). See the text for details.

**TABLE 5: Infrared Bands of Methylenebisoxo ( $\text{H}_2\text{COO}$ ) Species Adsorbed on Several Metal Oxides**

oxide	$\nu_{\text{as}}(\text{CH}_2)$	$\nu_{\text{s}}(\text{CH}_2)$	$\delta(\text{CH}_2)$	$\rho(\text{CH}_2)$	$\nu(\text{CO})$	ref
$\text{Ga}_2\text{O}_3$	2948	2845	nd	nd	1107	this work
$\text{TiO}_2$	2950	2868	1482	1113	1070	67
$\text{ZrO}_2$	2970	2870	1490	1117	1070	67
$\text{ThO}_2$	2960	2840	1495	1112	1070	67
$\text{CeO}_2$		2780		1170–80	1088	70
$\text{ZnAl}_2\text{O}_4$	2885	2770	1265	1160	1107	71
$\text{SnO}_2$				1153	1075	72

It can be noted in Figure 11 that the pair of signals at 2948 and 2845  $\text{cm}^{-1}$  is located at higher wavenumbers than those of methoxy groups and in a different position from those belonging to formate species (see also Figure S10 in the Supporting Information). Plausibly, surface  $\text{CH}_3\text{O}$  and  $\text{HCOO}$  species might react to give molecularly adsorbed methyl formate groups ( $\text{HCOOCH}_3$ ), originating these peaks at 2948 and 2845  $\text{cm}^{-1}$ . However, we can rule out this possibility according to the following arguments: (i) the desorption of  $\text{HCOOCH}_3$  to the gas phase was not detected in the TPSR-MS experiments; (ii) molecular  $\text{HCOOCH}_3$  species adsorbs on strong Lewis acid sites<sup>34</sup> and hardly remain bonded at such a high temperature (i.e., 623 K);<sup>33</sup> and (iii) even though the  $\text{HCOOCH}_3$  group exhibits IR signals in the  $\nu(\text{CH})$  region in very similar positions than those of the  $\text{CH}_3\text{O}$  and  $\text{HCOO}$  species, the former also has characteristic bands at 1700–1650  $\text{cm}^{-1}$  [ $\nu_{\text{as}}(\text{OCO})$ ], 1400–1380  $\text{cm}^{-1}$  [ $\delta(\text{CH})$ ], and  $\sim 1300$   $\text{cm}^{-1}$  [ $\nu_{\text{s}}(\text{OCO})$ ], none of which were discerned in spectrum B at 623 K.

On the contrary, several authors have reported the presence of  $\nu_{\text{as}}(\text{CH}_2)$ ,  $\nu_{\text{s}}(\text{CH}_2)$ , and  $\nu(\text{CO})$  modes at approximately 2950, 2850, and 1070  $\text{cm}^{-1}$  over a wide range of metal oxides, which have been attributed to the  $\text{H}_2\text{COO}$  species (see Table 5). Therefore, a reasonable assignment to the signals at 2948 and 2845  $\text{cm}^{-1}$  is the symmetric and asymmetric stretching mode of the C–H bond,  $\nu_{\text{as}}(\text{CH}_2)$ , and  $\nu_{\text{s}}(\text{CH}_2)$ , of methylenebisoxo or dioxymethylene ( $\text{H}_2\text{COO}$ ) species bonded to the gallia surface. Also, its [ $\nu(\text{CO})$ ] weak peak, at 1107  $\text{cm}^{-1}$ , can be distinguished in spectrum B of Figure 11.

**3.2.2. TPSR of Adsorbed Methanol- $d_3$ .** Two extra experiments of  $\text{CD}_3\text{OH}$  adsorption and surface reaction on a hydrogen activated  $\text{Ga}_2\text{O}_3$  samples were run, following the MS and FTIR signals to accomplish a deeper understanding of the methanol decomposition pathway on the surface of gallium oxide.

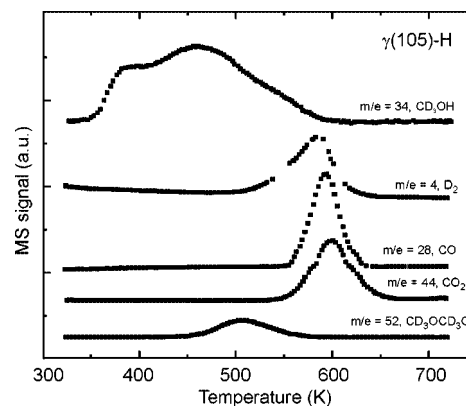


**Figure 12.** TPSR followed by mass spectrometry between 323 and 723 K after the adsorption of  $\text{CD}_3\text{OH}$  at 373 K on  $\gamma(105)\text{-O}$  (heating rate = 10  $\text{K min}^{-1}$ , 60  $\text{cm}^3 \text{He min}^{-1}$ ).

The MS results obtained by exposing the  $\gamma(105)\text{-H}$  sample at 373 K to pulses of  $\text{CD}_3\text{OH}$  were identical to those previously reported, that is, only nonadsorbed methanol ( $\text{CD}_3\text{OH}$ ) and desorption of water ( $\text{H}_2\text{O}$ ) from the surface were detected in the gas phase. The TPSR-MS evolution of the gaseous, molecular species at increasing temperatures is depicted in Figure 12. Deuterated methanol ( $\text{CD}_3\text{OH}$ ,  $m/e = 34$ ) and dimethyl ether ( $\text{D}_3\text{COCD}_3$ ,  $m/e = 52$ ) show desorption patterns similar to the  $\text{CH}_3\text{OH}$  and  $\text{CH}_3\text{OCH}_3$  traces presented in Figure 3, respectively. Partially deuterated dimethyl ether molecules ( $\text{CHD}_2\text{OCD}_3$ ,  $m/e = 51$ , and  $\text{CHD}_2\text{OCHD}_2$  and/or  $\text{CH}_2\text{DOCD}_3$ ,  $m/e = 50$ ) were also released to the gas phase. The oxidation products coming from the methanol- $d_3$  surface reaction, CO ( $m/e = 28$ ) and  $\text{CO}_2$  ( $m/e = 44$ ), were also released with peak temperatures at  $\sim 590$  and  $\sim 600$  K, that is, close to the ones registered after the TPSR of  $\text{CH}_3\text{OH}$ . Additionally, we were able to follow the thermal development of  $\text{D}_2$  ( $m/e = 4$ ), with a peak temperature at ca. 588 K.

Figure 13 shows the TPSR-IR spectra of adsorbed methanol- $d_3$  on  $\alpha(40)\text{-O}$ . Similarly to previous results, the concentration of  $\text{CD}_3\text{OH}_s$  species constantly decreased along the temperature ramp from 323 to 473 K, while  $\text{CD}_3\text{O}$  surface groups increased slightly from 323 to 373 K and, then, sharply decreased and disappeared at  $\sim 600$  K. The spectra from  $T > 423$  K show the development of several IR signals in the 1600–1300  $\text{cm}^{-1}$  region. The positions of these bands are shifted to lower wavenumbers with respect to those of the same set registered after the decomposition of  $\text{CH}_3\text{OH}$  (see, for example, Figure

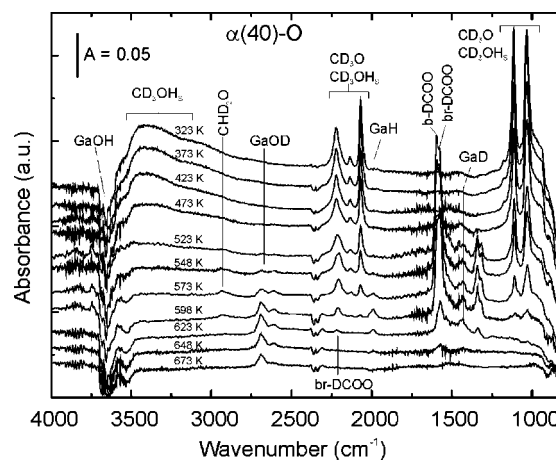


**Figure 13.** Infrared spectra during the TPSR of adsorbed  $\text{CD}_3\text{OH}$  on  $\alpha(40)\text{-O}$  (heating rate = 10  $\text{K min}^{-1}$ , 60  $\text{cm}^3 \text{He min}^{-1}$ ).

S7 in the Supporting Information), namely: (i) the couple of bands assigned to the symmetric and asymmetric OCO stretching modes of *m*-HCOO (1665 and 1305  $\text{cm}^{-1}$ ), *b*-HCOO (1600 and 1332  $\text{cm}^{-1}$ ), and *br*-HCOO (1575 and 1369  $\text{cm}^{-1}$ ) become slightly shifted approximately  $-7$  and  $-30$   $\text{cm}^{-1}$ , respectively; and (ii) the CH stretching mode IR for *b*- and *br*-HCOO (2915  $\text{cm}^{-1}$ ) is now situated at 2215  $\text{cm}^{-1}$ , that is,  $\nu(\text{CH})/\nu(\text{CD}) = 1.32$ , which is very close to the expected theoretical ratio, equal to 1.36. The CH bending modes for *b*-HCOO (1385  $\text{cm}^{-1}$ ) and *br*-HCOO (1355  $\text{cm}^{-1}$ ) should be shifted and located below the cutoff of gallia ( $\sim 1000$   $\text{cm}^{-1}$ ). Thus, Table 4 shows that the assignments of all these bands to formates are unambiguous, in accordance with the near agreement between the experimental and predicted shift of the band positions observed for their deuterated and hydrogenated counterparts.

From 523 K upward, a band at 1442  $\text{cm}^{-1}$  appears, which is assigned to the stretching mode of Ga-D surface species (again, the experimental  $\nu(\text{Ga-H})/\nu(\text{Ga-D}) = 1.38$ , in fair agreement with the expected 1.40 theoretical ratio). In addition, two new bands emerged at 2690 and 2610  $\text{cm}^{-1}$ , from about 523 K, attributed to OD groups bonded to gallium surface cations, that is,  $\text{DO-}\mu_2\text{-Ga}^{\text{VI}}$  and  $\text{DO-}\mu_3\text{-Ga}^{\text{VI}}$ , respectively.<sup>14</sup> The concentration of both the Ga-D and Ga-OD species increased up to 673 K.

Together with the appearance of the previous bands, H/D isotopic exchange between the deuterated adsorbates and the OH or H of the gallia surface occurred. This phenomenon is revealed by at least two observations in the TPSR-IR experiment; first, the rise of a peak at 1980  $\text{cm}^{-1}$  attributed to Ga-H species<sup>13</sup> at  $T > 548$  K; and second, a new, low intensity band at 2934  $\text{cm}^{-1}$  that is observed from 473 to 673 K, which can be attributed to the CH stretching mode of  $\text{CD}_2\text{HO}$  species, as follows. We exclude the H/D exchange between DCOO species with superficial hydroxyls or gallium-hydrogen groups (for example,  $\text{DCOO} + \text{H}_\text{s} \rightarrow \text{HCOO} + \text{D}_\text{s}$ ) because the bands corresponding to the CH vibrations of formates would be situated at 2992 and 2915–2895  $\text{cm}^{-1}$ , that is, in a different location from the 2934  $\text{cm}^{-1}$  measured wavenumber (see Table 4). Next, the H/D isotopic exchange between the  $\text{CD}_3\text{O}$  species and surface OH or H groups must also be considered. In this regard, Ouyang et al.<sup>72,73</sup> concluded that the methoxy species on  $\text{ZrO}_2$  exchanged the H atoms of the methyl group with the surface OD groups, in the 523–623 K temperature range, even in the absence of  $\text{D}_2(\text{g})$ . In other words, the reaction  $\text{CH}_3\text{O-M} + \text{DO-M} \rightarrow \text{CH}_2\text{DO-M} + \text{HO-M}$  (M, metallic cation) can take place. The  $\nu(\text{CH})$  mode of the methanol-*d*<sub>2</sub> molecule ( $\text{CD}_2\text{HOH}$ ) dissolved in chloroform is situated at 2920  $\text{cm}^{-1}$ , close to the 2960–2900  $\text{cm}^{-1}$  bands of  $\text{CD}_2\text{HOH}_\text{s}$  over activated  $\delta\text{-Al}_2\text{O}_3$ .<sup>23</sup> Therefore, because the H/D isotopic exchange between methoxy groups and surface OH species over metallic oxides can occur and the position of the  $\nu(\text{CH})$  mode corresponding to  $\text{CD}_2\text{HO}$  groups on metallic oxides is similar to the one reported here at 2934  $\text{cm}^{-1}$ , we suggest that the  $\text{CD}_2\text{HO}$  species on the gallia surface is generated by the H/D isotopic exchange between  $\text{CD}_3\text{O}$  and the remaining Ga-OH surface groups. Indeed, the partially deuterated dimethyl ether evolved to the gas phase during the TPSR-MS experiments (see above) confirms the presence of said hydrogenated–deuterated methoxy groups.

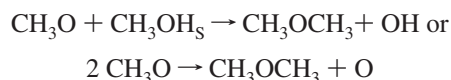
**3.2.3. Mechanism of Methanol Decomposition over Gallium Oxides.** We have shown that during the temperature increase in the TPSR experiments the concentration of  $\text{CH}_3\text{OH}_\text{s}$  species decreased steadily and vanished at  $\sim 500$  K. The desorption of  $\text{CH}_3\text{OH}$  at low temperature ( $T < 423$  K) is mainly due to

molecularly adsorbed methanol, whereas the high-temperature part of the desorption trace comes from the recombination between methoxy species and H atoms from hydroxyl groups. In general terms, the pattern of methanol desorption is very similar for all the gallia polymorphs.

Moreover, the  $\alpha$ -,  $\beta$ -, and  $\gamma$ - $\text{Ga}_2\text{O}_3$  polymorphs (activated under oxygen or hydrogen) showed a similar surface chemistry with respect to the decomposition of adsorbed methoxy species. The products distribution of the methanol decomposition can be used to determine the nature of the active sites on the surface of metal oxides.<sup>21,22</sup> So, the temperature-programmed surface reaction of adsorbed methanol/methoxy over gallium oxide showed the total absence of intermediate oxidation products such as formaldehyde, methylformate, or formic acid, which indicates that very active redox sites on the activated gallia surface are not available.<sup>21</sup>

However, the production of dimethyl ether by methanol dehydration is associated with the presence of acid sites. In our case, the selectivity to DME was marginal, which indicates just a low-to-moderate Lewis acidity of  $\text{Ga}_2\text{O}_3$ . On the other hand, though, Badlani and Wachs<sup>74</sup> reported that a sample of  $\text{Ga}_2\text{O}_3$  exhibited a 100% selectivity to dimethyl ether upon exposing the material to a  $\text{CH}_3\text{OH}/\text{O}_2/\text{He}$  flow mixture (molar ratio 6/13/81). Their case implies a significant Lewis acidity of the metallic oxide, in apparent contradiction with our results and conclusion. Nevertheless, it is clear that the discrepancy can be found in the dissimilar experimental conditions used in each situation. The decomposition of adsorbed methanol and methoxy species was studied here under temperature-programmed surface reaction conditions, that is, where only few oxycarbonaceous surface moieties were transformed over the surface of the gallia samples. In their case, because methanol was continuously fed into the reactor, the  $\text{CH}_3\text{OH}$  gaseous molecules could then continuously react with methoxy species bonded to acid sites to yield DME as the main product, even in the presence of  $\text{O}_2$ .

Unfortunately, no distinct IR signals related to adsorbed DME were detected during our TPSR-IR experiment, which is to be expected since the infrared spectroscopic distinction between DME and methoxy groups is very difficult<sup>74,75</sup> and, even more, the concentration of DME detected in the TPSR-MS was very low. In spite of that, it is certainly plausible to consider that the synthesis of DME might occur through the formation of a methyl intermediate bonded to a cation site, for example,  $\text{M-CH}_3$ . However, the identification of such a Ga- $\text{CH}_3$  entity is intricate too. Odom et al.<sup>75</sup> identified and assigned the IR signals of trimethylgallane–dimethylether [ $(\text{CH}_3)_3\text{GaO}(\text{CH}_3)_2$ ],  $\nu_{\text{as}}(\text{CH}_3) = 2953/2943$   $\text{cm}^{-1}$ ,  $\nu_{\text{s}}(\text{CH}_3) = 2897/2870$   $\text{cm}^{-1}$ ,  $\delta_{\text{as}}(\text{CH}_3) = 1424$   $\text{cm}^{-1}$ ,  $\delta_{\text{s}}(\text{CH}_3) = 1196/1188$   $\text{cm}^{-1}$ , and  $\rho(\text{CH}_3) = 747/728/653$   $\text{cm}^{-1}$ . Clearly, we are unable to identify IR bands belonging to the CH stretching or bending mode of Ga- $\text{CH}_3$  species because they would be overlapped to those of methoxy and adsorbed methanol entities. Still, it is possible to note that the ratio between the intensity of the bands in the 3000–2700  $\text{cm}^{-1}$  range and those in the 1150–1000  $\text{cm}^{-1}$  range, for example,  $[\nu(\text{CH}_3) + 2\delta(\text{CH}_3)]/\nu(\text{CO})$ , was fairly constant along the temperature ramp, which indicates that if some Ga- $\text{CH}_3$  was present its concentration would have been undetected under our experimental conditions. At this point, therefore, it seems logical to propose that the (low) DME formation can proceed either through the reaction between methanol and methoxy species or between two methoxy groups, as follows:



Now, as some of the remaining methoxy groups decomposed over the gallia surface to give CO(g) or CO<sub>2</sub>(g), at  $T > 550$  K, we can examine step-by-step this decomposition sequence of methoxy groups over the gallia surface according to the evidence supplied by FTIR and MS.

First, a careful analysis of the IR spectra collected during the TPSR experiments allowed us to identify the presence of the methylenebisoxo species, which is thought of as an intermediate in the dehydrogenation of methoxy to formate.<sup>23,33,34</sup> The thermal evolution of the surface concentration of H<sub>2</sub>COO species could not be determined, because we were unable to precisely define or solve its overlapped IR bands. Nevertheless, H<sub>2</sub>COO species have been experimentally identified and proposed as an intermediate in the partial oxidation and decomposition of methanol and formaldehyde over a wide range of metal oxides.<sup>34,67</sup> In particular, the oxidation of methanol over vanadia–titania has been rationalized as a stepwise mechanism where methanol reacts with V–OH to form methoxy, which is then oxidized to  $\pi$ -coordinated formaldehyde and further attacked—nucleophilically—by a basic surface oxygen to form methylenebisoxo. The latter can be finally oxidized to formate, which can in turn react with methanol to give methylformate or with water to produce formic acid or can decompose to carbon oxides.<sup>21,22,33,34</sup> A similar sequence from methoxy to methylenebisoxo species was observed during the decomposition of methanol over ZrO<sub>2</sub>(110) by HREELS.<sup>76</sup> The vibration frequencies of H<sub>2</sub>COO were observed on the ZrO<sub>2</sub>(110) plane, a surface with oxygen atoms in the first layer available to produce the nucleophilic attack on methoxy groups.<sup>76</sup> By contrast, methylenebisoxo species were not synthesized on the ZrO<sub>2</sub>(100) surface, that is, where oxygen atoms are present in the second surface layer.<sup>76</sup> Furthermore, the methoxy groups adsorbed on reduced ceria–zirconia mixed oxides could produce H<sub>2</sub>COO or polyoxymethylene species at room temperature after O<sub>2</sub> doses were added to the sample.<sup>56</sup>

Therefore, there is enough experimental evidence in the literature to visualize the formation of methylenebisoxo species as due to the nucleophilic attack by surface lattice oxygen atoms to the methoxy group and the concerted release of a hydrogen atom, probably forming a OH, with a progressive recovery of the Ga–OH surface groups, as it is observed in the TPSR-IR spectra, which show the restoration of the  $\nu(\text{OH})$  band when the temperature is increased. Nonetheless, methylenebisoxo groups seem to be very reactive and to promptly decompose to formate species.

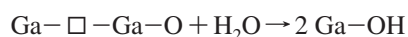
The thermal evolution of formate species could be followed by FTIR from  $\sim 500$  to 650 K (Figures 8–10). Formate groups decompose rather easily over metal oxides according to the reversible reaction:  $\text{HCOO} \leftrightarrow \text{CO} + \text{OH}$ .<sup>23</sup> Indeed, TPSR-IR showed that a progressive recovery of the Ga–OH(D) surface groups also occurred above 573 K, that is, where formate started to decompose and, accordingly, the release of CO to the gas phase was detected by MS. Additionally, the nonstoichiometric decomposition of HCOO due to the desorption of CO<sub>2</sub> and the detection of Ga–H(D) surface species was also observed.

It was recently reported by some of us that formate species can be synthesized over the gallia surface either (i) by the insertion of CO on Ga–OH sites<sup>69</sup> (at  $T > 473$  K), giving m-HCOO, b-HCOO, and br-HCOO, which further decompose to Ga–H and CO<sub>2</sub> at temperatures higher than 573 K; or (ii) by the reaction between Ga–H species with carbonates formed

after the adsorption of CO<sub>2</sub>.<sup>8</sup> Therefore, we can conclude that during the TPSR of adsorbed methanol, formate groups decompose at temperatures higher than 573 K to either CO and Ga–OH or CO<sub>2</sub> and Ga–H. The absence of surface carbonates as intermediates, prior to the release of CO<sub>2</sub>(g), is expected due to the low thermal stability of the carbonate groups on the gallia surface.<sup>14</sup>

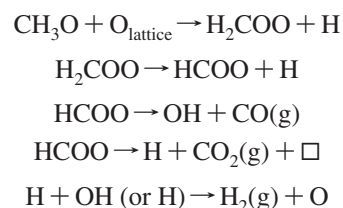
Although the TPSR-IR results allowed us to distinguish among three kinds of formate groups—m-HCOO, b-HCOO, and br-HCOO—, it is not an easy task to determine which of these surface species generates CO or CO<sub>2</sub>. Recent theoretical results on the stability of the formate species produced by the insertion of CO on a hydroxylated  $\beta$ -Ga<sub>2</sub>O<sub>3</sub> (100) using DFT calculations, show that four types of formates [mono-, di- (bidentate and bridged), and tricoordinate] can interconvert to one another, with the bridged species being the most stable.<sup>68</sup> Among them, monodentate formate was found to decompose to CO<sub>2</sub> with the lowest activation energy, through lattice oxygen abstraction and the formation of Ga–H on the surface.<sup>68</sup> Then, we can suggest that m-HCOO can proceed by parallel reaction pathways to CO(g) and OH, or CO<sub>2</sub>(g) and H, with the selectivity to the gaseous products being dependent on the activation barriers of each step.

It is also worth noticing that the reaction pathway of formate decomposition to CO<sub>2</sub> should involve the abduction of lattice oxygen, leaving a surface oxygen vacancy next to gallium cations (Ga–□). These vacancy sites could be rapidly replenished by water molecules from the gas phase. Actually, during the TPSR-MS experiments a suppression of the intensity of the water signal was registered in the same range of temperature where the CO<sub>2</sub> was produced (see for example Figures 3 and 4). Hence, we can suggest that part of the water desorbed from the gallia surface reacts with the Ga–□ to refill the oxygen vacancy, as follows:



The TPSR-MS experiment of methanol-*d*<sub>3</sub> over  $\gamma$ -Ga<sub>2</sub>O<sub>3</sub> (Figure 12) neatly showed that the release of D<sub>2</sub> to the gas phase started at  $T > 500$  K, that is, from the pronounced decrease of the methanol band in the MS spectrum. Some of us have already reported that Ga–H(D) and Ga–OH(OD) species can recombine to give H<sub>2</sub> (D<sub>2</sub>) and Ga–O–Ga under heating.<sup>13</sup>

According to the previous observations and analyses, the decomposition of methoxy species over the gallia surface can be summarized as follows,



where □ stands for an oxygen vacancy.

The high mobility of surface H was revealed by the detection of H/D scrambling on Ga [Ga–H(D)] and Ga–O [Ga–OH(D)] sites. This last observation points to an improvement of the probability for a fast release of H<sub>2</sub>(g), via a reverse spillover mechanism, when noble metal particles (for example, palladium) are dispersed onto the surface. It seems then that, while methanol decomposes over the gallia surface to give carbon oxides, the cofeeding of water could regenerate the surface oxygen vacancies, and noble metal particles would be responsible for a fast liberation of molecular hydrogen. Therefore, a good performance



of gallium-oxide-supported noble metal catalyst for the production of hydrogen from the steam reforming of methanol can be envisaged.<sup>12</sup>

Finally, this study of methanol decomposition on gallia sheds additional light on the mechanism of methanol synthesis from carbon dioxide and hydrogen mixtures. A bifunctional mechanism was previously proposed using Pd/ $\beta$ -Ga<sub>2</sub>O<sub>3</sub>;<sup>12</sup> oxycarbonaceous species evolve on the surface of the oxide, and its hydrogenation is provided by atomic hydrogen from the palladium metal crystallites.<sup>11</sup> Therefore, gaseous CO<sub>2</sub> is weakly adsorbed over the gallia surface, giving carbonate and bicarbonate groups. These (bi)carbonates react with surface H, sequentially producing (monodentate)formate, methylenbisoxo, and methoxy groups. However, methylenbisoxo species were not detected neither over the pure support nor on the Pd/Ga<sub>2</sub>O<sub>3</sub> catalyst after running temperature-programmed reaction experiments in the IR cell with a flowing mixture of CO<sub>2</sub>/H<sub>2</sub>.<sup>8</sup> Now, our data show that H<sub>2</sub>COO can be generated from methoxy decomposition on pure gallia, most likely owing to the more abundant surface methoxy concentration in these experiments.

#### 4. Conclusions

Insights regarding methanol chemisorption and surface reaction over bulk gallium oxides ( $\alpha$ -,  $\beta$ -, and  $\gamma$ -phases) were obtained through the investigation, by mass spectrometry and IR spectroscopy, of the surface intermediates and desorption products during the surface reaction of preadsorbed methoxy species.

CH<sub>3</sub>OH adsorbs on gallia at 373 K, producing a stable layer of chemisorbed methoxy species. Methanol is adsorbed molecularly (CH<sub>3</sub>OH<sub>S</sub>) and dissociatively over the gallium oxide surface at this temperature regardless of the polymorph and the pretreatment procedure (under molecular oxygen or hydrogen, at 723 K). In the first case, a 200 cm<sup>-1</sup> shifting of the  $\nu$ (OH) band of CH<sub>3</sub>OH<sub>S</sub> species, as compared to gaseous methanol, is indicative of a relatively strong hydrogen-bridged interaction between the CH<sub>3</sub>OH<sub>S</sub> and the basic O<sup>2-</sup> sites of the gallium oxide surface. Some of the gaseous methanol also reacts with the GaOH groups, to give CH<sub>3</sub>O surface species and water. Both oxycarbonaceous species could be spectroscopically distinguished mainly by their partially overlapped  $\nu$ (CO) peaks, at 1030 and 1070 cm<sup>-1</sup>.

After being heated from 323 to 723 at 10 K min<sup>-1</sup> under flowing He, methanol, dimethyl ether, carbon monoxide, and carbon dioxide evolved to the gas phase from the adsorbed methanol/methoxy surface species. Methanol, from either CH<sub>3</sub>OH<sub>S</sub> or a recombination of CH<sub>3</sub>O and OH surface groups, desorbed up to 573 K, whereas dimethyl ether formation—in the 473–573 K temperature range—is suggested to proceed through the reaction between CH<sub>3</sub>OH<sub>S</sub> and CH<sub>3</sub>O or between two CH<sub>3</sub>O species. Part of the residual methoxy species further decomposed to CO and CO<sub>2</sub> at temperatures higher than 550 K. The decomposition sequence proposed to this last methoxy oxidation procedure involves (i) the reaction between CH<sub>3</sub>O species and an oxygen lattice, to give methylenbisoxo (H<sub>2</sub>COO) groups, followed by (ii) the formation of formate species, (iii) which finally decompose to either CO and OH or CO<sub>2</sub> and H, leading to an additional oxygen vacancy in the last case.

**Acknowledgment.** The financial support of the Consejo Nacional de Investigaciones Científicas y Técnicas (CONICET) and the Agencia Nacional para la Promoción de la Ciencia y Tecnología (ANPCyT) is gratefully acknowledged. S.E.C., M.A.B., and A.L.B. thank the Universidad Nacional del Litoral

(UNL) for its continued support. L.E.B. thanks the Universidad Nacional de La Plata for the Grant No. 11X-378.

**Supporting Information Available:** Infrared spectrum of a gallia sample activated in deuterium (Figure S1), IR spectra of the coadsorption of CO<sub>2</sub> and CH<sub>3</sub>OH on gallia (Figure S2), additional TPSR-MS (Figures S3–S6), and TPSR-IR results (Figures S7–S10). This material is available free of charge via the Internet at <http://pubs.acs.org>.

#### References and Notes

- (1) Ono, Y. *Catal. Rev.-Sci. Eng.* **1992**, *34*, 179.
- (2) Moreno, J. A.; Poncelet, G. J. *Catal.* **2001**, *203*, 453.
- (3) Shimizu, K.; Satsuma, A.; Hattori, T. *Appl. Catal., B* **1998**, *16*, 319.
- (4) Haneda, M.; Kintaichi, Y.; Hamada, H. *Appl. Catal., B* **1999**, *20*, 289.
- (5) Haneda, M.; Kintaichi, Y.; Shimada, H.; Hamada, H. *J. Catal.* **2000**, *192*, 137.
- (6) Fujitani, T.; Saito, M.; Kanai, Y.; Watanabe, T.; Nakamura, J.; Uchijima, T. *Appl. Catal., A* **1995**, *125*, L199.
- (7) Bonivardi, A. L.; Chiavassa, D. L.; Querini, C. A.; Baltanás, M. A. *Stud. Surf. Sci. Catal.* **2000**, *130D*, 3747.
- (8) Collins, S. E.; Baltanás, M. A.; Bonivardi, A. L. *J. Catal.* **2004**, *226*, 410.
- (9) Iwasa, N.; Mayanagi, T.; Ogawa, N.; Sakata, K.; Takezawa, N. *Catal. Lett.* **1998**, *54*, 119.
- (10) Iwasa, N.; Mayanagi, T.; Nomura, W.; Arai, M.; Takezawa, N. *Appl. Catal., A* **2003**, *248*, 153.
- (11) Collins, S. E.; Chiavassa, D. L.; Baltanás, M. A.; Bonivardi, A. L. *Catal. Lett.* **2005**, *103*, 83.
- (12) Collins, S. E.; Baltanás, M. A.; Bonivardi, A. L. *Appl. Catal., A* **2005**, *295*, 126.
- (13) Collins, S. E.; Baltanás, M. A.; Bonivardi, A. L. *Langmuir* **2005**, *21*, 962.
- (14) Collins, S. E.; Baltanás, M. A.; Bonivardi, A. L. *J. Phys. Chem. B* **2006**, *110*, 5498.
- (15) Lavalley, J. C.; Daturi, M.; Montouillout, V.; Clet, G.; Otero Areán, C.; Rodríguez Delgado, M.; Sahibed-Dinde, A. *Phys. Chem. Chem. Phys.* **2003**, *5*, 1301.
- (16) Rodríguez Delgado, M. R.; Morterra, C.; Cerrato, G.; Magnacca, G.; Otero Areán, C. *Langmuir* **2002**, *18*, 10255.
- (17) Rodríguez Delgado, M.; Otero Areán, C. *Mater. Lett.* **2003**, *57*, 2292.
- (18) Vimont, A.; Lavalley, J. C.; Sahibed-Dine, A.; Otero Areán, C.; Rodríguez Delgado, M.; Daturi, M. *J. Phys. Chem. B* **2005**, *109*, 9656.
- (19) Ingle, J. D.; Crouch, S. R. *Spectrochemical Analysis*, 1st ed.; Prentice Hall: Upper Saddle River, NJ, 1988; p 211.
- (20) Briand, L. E.; Farneth, W. E.; Wachs, I. E. *Catal. Today* **2000**, *62*, 219.
- (21) Tatibouët, J. M. *Appl. Catal., A* **1997**, *148*, 213.
- (22) Wachs, I. E.; Jehng, J.-M.; Ueda, W. *J. Phys. Chem. B* **2005**, *109*, 2275.
- (23) Busca, G.; Rossi, P. F.; Lorenzelli, V.; Benaissa, M.; Travert, J.; Lavalley, J.-C. *J. Phys. Chem.* **1985**, *89*, 5433.
- (24) Branda, M. M.; Collins, S. E.; Castellani, N. J.; Baltanás, M. A.; Bonivardi, A. L. *J. Phys. Chem. B* **2006**, *110*, 11487.
- (25) Clarke, D. B.; Bell, A. T. *J. Catal.* **1995**, *154*, 314.
- (26) Clarke, D. B.; Lee, D.-K.; Sandoval, M. J.; Bell, A. T. *J. Catal.* **1994**, *150*, 81.
- (27) Millar, G. J.; Rochester, C. H.; Waugh, K. C. *J. Chem. Soc. Faraday Trans.* **1991**, *87*, 2785.
- (28) Raskó, J.; Bontovics, J.; Solymosi, F. *J. Catal.* **1994**, *146*, 22.
- (29) Cabilla, G.; Bonivardi, A. L.; Baltanás, M. A. *J. Catal.* **2001**, *201*, 213.
- (30) Derouault, J.; Le Calve, J.; Forel, M. T. *Spectrochim. Acta* **1972**, *28*, 359.
- (31) Lavalley, J. C.; Sheppard, N. *Spectrochim. Acta* **1972**, *28*, 2091.
- (32) Bellamy, L. J. In *Advances in Infrared Groups Frequencies*; Chapman and Hall: London, 1968; Chap. 1.
- (33) Busca, G.; Elmi, A.; Forzatti, P. *J. Phys. Chem.* **1987**, *91*, 5263.
- (34) Busca, G. *Catal. Today* **1996**, *27*, 457.
- (35) Burcham, L. G.; Briand, L. E.; Wachs, I. E. *Langmuir* **2001**, *17*, 6164.
- (36) Burcham, L. G.; Briand, L. E.; Wachs, I. E. *Langmuir* **2001**, *17*, 6175.
- (37) Burcham, L. J.; Badlani, M.; Wachs, I. E. *J. Catal.* **2001**, *203*, 104.
- (38) Lavalley, J. C. *Catal. Today* **1996**, *27*, 377.
- (39) Chesters, M. A.; McCash, E. M. *Spectrochim. Acta* **1987**, *43*, 1630.
- (40) Huberty, J. S.; Madix, R. J. *Surf. Sci.* **1996**, *360*, 144.

- (41) Uvdal, P.; Weldon, M. K.; Friend, C. M. *Phys. Rev. B* **1994**, *50*, 12258.
- (42) Asmundsson, R.; Uvdal, P. *J. Chem. Phys.* **2000**, *112*, 366.
- (43) Andersson, M. P.; Uvdal, P.; MacKerell, A. D. *J. Chem. Phys. B* **2002**, *106*, 5200.
- (44) Sim, W. S.; Gardner, P.; King, D. A. *J. Phys. Chem.* **1995**, *99*, 16002.
- (45) Brito de Barros, R.; García, A. R.; Ilharco, L. M. *Surf. Sci.* **2003**, *532–535*, 185.
- (46) Pinto, A. S. S.; Brito de Barros, R.; Cordeiro, M. N. D. S.; Gomes, J. A. N. F.; Garcia, A. R.; Ilharco, L. M. *Surf. Sci.* **2004**, *566–568*, 965.
- (47) Brito de Barros, R.; García, A. R.; Ilharco, L. M. *Surf. Sci.* **2004**, *572*, 277.
- (48) Mudalige, K.; Trenary, M. *J. Phys. Chem. B* **2001**, *105*, 3823.
- (49) Herzberg, G. *Infrared and Raman Spectra of Polyatomic Molecules*, In *Molecular Spectra and Molecular Structure II*; Van Nostrand Reinhold: New York, 1945; p 334.
- (50) Giguere, J.; Overned, J. *Spectrochim. Acta* **1976**, *32A*, 241.
- (51) Serrallach, A.; Meyer, R.; Gunthard, H. H. *J. Mol. Spectrosc.* **1974**, *52*, 94.
- (52) Briand, L. E. in *Metal Oxides: Chemistry and Applications*; García Fierro, J. L. Ed.; CRC Taylor & Francis: Boca Raton, FL, 2006; Chap. 11.
- (53) Binet, C.; Badri, A.; Lavalley, J.-C. *J. Phys. Chem.* **1994**, *98*, 6398.
- (54) Binet, C.; Daturi, M.; Lavalley, J.-C. *Catal. Today* **1999**, *50*, 207.
- (55) Daturi, M.; Binet, C.; Lavalley, J.-C.; Galtayries, A.; Sporken, R. *Phys. Chem. Chem. Phys.* **1999**, *1*, 5717.
- (56) Binet, C.; Daturi, M. *Catal. Today* **2001**, *70*, 155.
- (57) Collins, S. E.; Baltanás, M. A.; Bonivardi, A. L. *J. Catal.* **2002**, *211*, 252.
- (58) Lamotte, J.; Morávek, V.; Bensitel, M.; Lavalley, J. C. *React. Kinet. Catal. Lett.* **1988**, *36*, 113.
- (59) Ouyang, F.; Kondo, J. N.; Maruya, K.; Domen, K. *J. Phys. Chem. B* **1997**, *101*, 4867.
- (60) Lamotte, J.; Saur, O.; Lavalley, J. C.; Busca, G.; Rossi, P. F.; Lorenzelli, V. *J. Chem. Soc. Faraday Trans.* **1986**, *82*, 3019.
- (61) Jung, K. T.; Bell, A. T. *J. Catal.* **2001**, *204*, 339.
- (62) Busca, G.; Lorenzelli, V. *Mater. Chem.* **1982**, *7*, 89.
- (63) Gibson, D. H. *Coord. Chem. Rev.* **1999**, *185*, 335.
- (64) Sun, Q.; Liu, C.; Pan, W.; Zhu, Q.; Deng, J. F. *Appl. Catal., A* **1998**, *171*, 301.
- (65) Pokrovski, K.; Jung, K. T.; Bell, A. T. *Langmuir* **2001**, *17*, 4297.
- (66) Gao, L. Z.; Au, C. T. *J. Catal.* **2000**, *189*, 1.
- (67) Busca, G.; Lamotte, J.; Lavalley, J. C.; Lorenzelli, V. *J. Am. Chem. Soc.* **1987**, *109*, 1491.
- (68) Calatayud, M.; Collins, S. E.; Baltanás, M. A.; Bonivardi, A. L. Submitted to *Phys. Chem. Chem. Phys.*
- (69) Collins, S. E.; Baltanás, M. A.; Bonivardi, A. L. *J. Mol. Catal. A: Chem.* **2008**, *281*, 73.
- (70) Li, C.; Domen, K.; Maruya, K.; and Onish, T. *J. Catal.* **1993**, *141*, 540.
- (71) Idriss, H.; Hindermann, J. P.; Kieffer, R.; Kiennemann, A.; Vallet, A.; Chauvin, C.; Lavalley, J. C.; Chaumette, P. *J. Mol. Catal.* **1987**, *42*, 205.
- (72) Ouyang, F.; Yao, S.; Tabata, K.; Suzuki, E. *Appl. Surf. Sci.* **2000**, *158*, 28.
- (73) Ouyang, F.; Kondo, J. N.; Maruya, K.; Domen, K. *J. Chem. Soc., Faraday Trans.* **1997**, *93*, 169.
- (74) Badlani, M.; Wachs, I. E. *Catal. Lett.* **2001**, *75*, 137.
- (75) Odom, J. D.; Wasacz, F. M.; Sullivan, J. F.; During, J. R. *J. Raman Spectrosc.* **1981**, *11*, 469.
- (76) Dilara, P. A.; Vohs, J. M. *Surf. Sci.* **1994**, *321*, 155.

JP801252D